



ELSEVIER

Progress in Biophysics & Molecular Biology 86 (2004) 45–76

*Progress in*  
**Biophysics  
& Molecular  
Biology**

www.elsevier.com/locate/pbiomolbio

# Transcriptional control networks of cell differentiation: insights from helper T lymphocytes

Luca Mariani<sup>a</sup>, Max Löhning<sup>b</sup>, Andreas Radbruch<sup>c</sup>, Thomas Höfer<sup>a,\*</sup>

<sup>a</sup>*Department of Theoretical Biophysics, Institute of Biology, Humboldt University Berlin, Invalidenstrasse 42, 10115 Berlin, Germany*

<sup>b</sup>*Institute of Experimental Immunology, University Hospital Zurich, Schmelzbergstrasse 12, 8091 Zurich, Switzerland*

<sup>c</sup>*German Arthritis Research Center Berlin, Schumannstrasse 21/22, 10117 Berlin, Germany*

---

## Abstract

Coordinated programs of gene expression during cell differentiation can be controlled by master transcription factors. The differentiation of helper T (Th) lymphocytes during the immune response has been shown to occur along alternative pathways designated as Th1 and Th2. Induction of the Th1 and Th2 pathways is associated with the conversely regulated expression of the master factors T-bet and GATA-3, respectively. Both autoactivation and inhibition of GATA-3 play a crucial role in this process. We develop mathematical models of the underlying regulatory networks to provide a framework for the analysis of experimental data. Modeling concepts for gene expression dynamics are introduced, and paradigms for the behavior of gene-regulatory networks are reviewed. A mechanistic model for the regulation of GATA-3 in Th cells is developed that accounts for autoactivation and regulation by external differentiation signals. This system works as a bistable switch that enables the triggering of a differentiation program by transient inductive signals. GATA-3 inhibitors (such as FOG-1 and ROG) modulate GATA-3 expression by yet unidentified mechanisms. Three potential modes of inhibition, sequestration by a binding protein, repression of basal transcription, and repression of autoactivation, are predicted to have distinct, and strongly concentration-dependent, regulatory effects on GATA-3 dynamics. Based on these results, we develop a model for the cross-regulation of the alternative Th1 and Th2 differentiation programs which are governed by the dynamics of T-bet and GATA-3, respectively. The steady states of this model correlate with naïve, Th1-polarized, and Th2-polarized phenotypes. Our analysis makes predictions on the stability of the Th1 and Th2 programs and raises questions on the relation between transcription factor regulation and epigenetic determination in cell differentiation.

© 2004 Elsevier Ltd. All rights reserved.

---

\*Corresponding author. Tel.: +49-30-2093-8592/8698; fax: +49-30-2093-8813.

E-mail address: thomas.hoefler@biologie.hu-berlin.de (T. Höfer).

## 1. Introduction

A multicellular organism is comprised of multiple cell types that differentiate from a pluripotent progenitor cell. The developmental processes involved have fascinated bioscientists from many different disciplines, e.g., developmental biologists and immunologists, with interests in different, specialized cell types. Studies in recent years have revealed common mechanisms underlying cell differentiation in the developmental processes. Alterations in the expression pattern and ratio of certain transcription factors have been shown to be critical for, and instructive in, the acquisition of certain cell phenotypes. Some of these transcription factors act as master transcription factors controlling the expression of several genes that form part of a developmental program. The actions of the transcription factors on the target genes may be positive, activating transcription, and also negative, inhibiting transcription. Inhibitory effects are often exerted on genes involved in the acquisition of alternative developmental programs, whereas expression of those genes that contribute to the maintenance of the initiated program are selectively enhanced. However, positive and negative regulatory interactions between transcription factors may form complex networks. The understanding of the network behavior and the prediction of the effects of individual interactions in such networks requires their quantitative description in terms of mathematical models. In this paper, we focus on an experimental model for cell differentiation in the immune system: the acquisition of cytokine memory in T lymphocytes. On the basis of recent experimental work that has identified master transcription factors and regulatory mechanisms, we develop a series of mathematical models and discuss their predictions.

Cytokines are signaling proteins that are secreted and sensed by a wide range of cell types including the cells of the immune system. Binding of cytokines to their receptors activates regulators of gene expression, such as signal transducers and activators of transcription (Stat) proteins. During the immune response, helper T (Th)<sup>1</sup> lymphocytes exert regulatory functions through cytokine production (Fig. 1). Th cells can express different sets of cytokines that mediate specific immunological functions. For example, the so-called Th2 cytokines, interleukin (IL) 4, IL-5, and IL-13, synergistically contribute to the establishment of a predominantly humoral, antibody-mediated immune response, which is most effective against extracellular pathogens. However, these cytokines are also critically involved in the immune pathology of allergy and asthma. In contrast, Th1 cytokines such as interferon- $\gamma$  (IFN- $\gamma$ ) predominantly activate cell-mediated responses, which are appropriate against intracellular pathogens, but are also involved in autoimmune pathologies (for a review, see Abbas et al., 1996; Murphy and Reiner, 2002).

In general, cytokine expression in Th cells is transient and depends on stimulation via the T cell receptor (TCR) for antigen. The question which cytokines are expressed upon Th cell stimulation is decided based on the respective differentiation lineage of the Th cell. Cytokine signals present during the initial activation of a naïve cell by antigen presentation act as inducers by driving differentiation programs associated with the distinct sets of cytokines and cell surface receptors. Potent inducers are IL-4 for Th2 cytokines and IL-12 for Th1 cytokines (Fig. 1). Interestingly,

---

<sup>1</sup> Abbreviations: IFN- $\gamma$ , interferon- $\gamma$ ; IL, interleukin; Stat, signal transducer and activator of transcription; TCR, T cell receptor; Th lymphocyte, helper T lymphocyte.

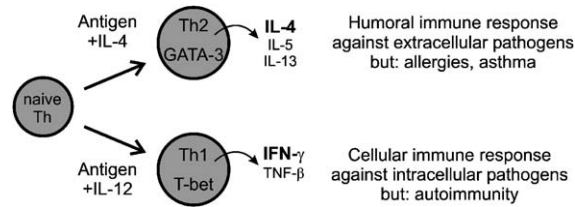


Fig. 1. Cytokine memory in Th lymphocytes. During their first encounter with antigen, Th lymphocytes can differentiate into distinct cytokine-producing phenotypes. Extreme points of differentiation are, on the one hand, Th1 cells that produce IFN- $\gamma$  and activate primarily the cellular immune response, and, on the other, Th2 cells that produce IL-4, IL-5 and IL-13, thereby activating B cells and antibody production. Th cell differentiation can be induced by cognate antigenic stimuli and appropriate differentiation signals: IL-12 (and IFN- $\gamma$ ) for the Th1 pathway, and IL-4 for the Th2 pathway. On secondary challenges with antigen, the cells recall their acquired cytokine pattern also in the absence of differentiation signals—they exhibit cytokine memory. Both in vitro and in vivo, the master transcription factors T-bet and GATA-3 are differentially upregulated in Th1 and Th2 cells, respectively, and have been shown to be crucial for the establishment of cytokine memory. Pathological Th1 and Th2 responses are associated with autoimmune disorders and allergies, respectively.

once a Th cell has been stimulated in this manner, it does not require the inducing IL-4 or IL-12 signals any more, but upon re-stimulation re-expresses those cytokines that it was primed to express during its primary activation. Thus a primed, differentiated Th cell has developed a memory for the expression of a certain set of cytokines. This phenomenon is referred to as cytokine memory (Löhning et al., 2002).

Memory for expression of specific cytokines is established and maintained on at least two levels. The expression of the master transcription factors GATA-3 and T-bet is selectively upregulated in Th cells by Th2-polarizing conditions (presentation of cognate antigen and IL-4) and Th1-polarizing conditions (antigen presentation and IL-12), and differential expression is maintained in polarized Th2 and Th1 cells, respectively (Zheng and Flavell, 1997; Szabo et al., 2000). GATA-3 expression has been found to be autoactivated, and high GATA-3 levels could thus be stably transmitted to daughter cells (Ouyang et al., 2000; Höfer et al., 2002). After this discovery, several factors have been shown to repress GATA-3 (Zhou et al., 2001; Kurata et al., 2002; Komine et al., 2003; Kusam et al., 2003), thus reinforcing the notion that inhibitory transcriptional regulation is also involved in Th1 and Th2 cell differentiation. On the level of DNA, modifications of cytokine genes and their regulatory elements have been reported. These include chromatin rearrangements and changes in histone acetylation and DNA methylation, which are believed to alter the accessibility of the DNA for the transcriptional machinery. These may act as epigenetic modifications that are passed on to the daughter cell generation and would thereby take part in the maintenance of cytokine memory (for a review, see Löhning et al., 2002).

Currently, the regulation of the master transcription factors is more clearly defined than the regulation of DNA modifications, and therefore we focus our modeling on the former. To provide an appropriate background for the modeling also to non-experts in the field, we begin with a review of the mathematical framework used to describe the dynamics of gene expression, the methods of analysis, and fundamental results. We then turn to specific models of the Th1/Th2 regulatory networks, proceeding from a model of GATA-3 activation in Th2 differentiation to

inclusion of GATA-3 inhibitors, and, finally, to a quantitative study of two alternative network models proposed for Th1/Th2 cross-regulation.

## 2. Concepts for modeling of gene expression

In this section, we give an introduction into the mathematical modeling of gene expression. We focus on models that predict measurable quantities, such as mRNA copy number and protein concentration (for other approaches, we refer to the literature, e.g., [Thomas et al., 1995](#); [de Jong, 2002](#)). Among the biochemical processes in the cell, gene transcription appears to be particularly prone to the influence of molecular fluctuations, since the number of molecules involved can be rather low. Typically there are one or two DNA templates, and some transcription factors can occur at very low concentration. However, molecular fluctuations generally do not appear to override the tight regulation of gene expression (e.g., [Cosma, 2002](#)). Therefore, we begin by introducing models of deterministic gene regulation, outline their methods of analysis, and discuss their results for regulatory feedback systems. In the final part of this section, molecular fluctuations are considered explicitly. Using a stochastic model of transcription, conditions are delineated under which such fluctuations have negligible impact on gene regulation. However, the model also shows that fluctuations may cause behavior that cannot be captured by a deterministic description.

### 2.1. Deterministic description of gene expression

The variables of primary interest in a quantitative description of gene expression are the number of mRNA copies of a given gene and the number of protein molecules. The cellular concentrations of mRNA and protein change in time according the balance equations

$$\begin{aligned} \frac{d}{dt}[\text{mRNA}] &= v_{\text{transcription}} - v_{\text{mRNA degradation}}, \\ \frac{d}{dt}[\text{protein}] &= v_{\text{translation}} - v_{\text{protein degradation}}, \end{aligned} \quad (2.1)$$

where the  $v$ 's denote the rates of transcription, translation, and degradation as indicated. Particularly in prokaryotes, cell cycling can be so rapid that mRNA and protein dilution due to growth and cell division may become more important than degradation. However, in view of the later application of the model to a eukaryotic system, we will not consider such effects. There may be additional levels of regulation, including mRNA processing, mRNA export from the nucleus, posttranslational protein modifications, such as phosphorylation, and protein transport through subcellular compartments. These can readily be accounted for in more detailed models. Particularly in eukaryotes, intricate mechanisms for regulating the accessibility of genes to the transcription machinery have evolved. The underlying dynamics of chromatin structure remain to be studied by quantitative modeling.

The first step of setting up a model of a specific system will be to establish how the rates of transcription, translation, and mRNA and protein degradation depend on the concentrations of mRNA, protein, and regulator molecules. The majority of known regulators in gene expression

control transcription. The rate of mRNA synthesis is determined by the rate of transcription initiation, and the efficiencies of elongation and RNA processing. Most of the regulatory machinery targets the initiation step, so that we take the transcription rate to be equal to the initiation rate and neglect any loss of transcript in transcription and RNA processing. Transcription initiation is controlled by regulatory proteins that control the accessibility of the promoter to the general transcription machinery and organize its assembly (e.g., Cosma, 2002). Thus we define the *state of a gene* according to which gene-specific and general transcription factors are bound (Fig. 2). The rate of transcription initiation from any particular state will depend on how well RNA polymerase is recruited to the promoter. RNA polymerase recruitment and initiation have recently begun to be studied in vivo (Dundr et al., 2002; Kimura et al., 2002).

To formalize this concept, we enumerate the possible states of a given gene by  $s=0, \dots, S$  and denote the probability to be in state  $s$  by  $x_s$ , and the corresponding transcription rate by  $v_s$ . The average rate of transcription is then

$$v_{\text{transcription}} = \sum_{s=0}^S x_s v_s. \tag{2.2}$$

A state  $s$  is characterized by how many molecules of each factor are bound, denoted by  $n_{i,s} \geq 0$  for the factors enumerated by  $i = 1, \dots, N$ . If one assumes that the binding equilibria of the transcription factors are attained rapidly, the general expression for the probability of a state  $x_s$  relative to the probability to find an empty gene reads

$$\gamma_s(F_1, \dots, F_N) := \frac{x_s}{x_0} = e^{-\Delta G_{0,s}/RT} \prod_{i=1}^N \left( \frac{F_i}{F_{i,0}} \right)^{n_{i,s}}, \tag{2.3}$$

Binding state	$s$	Probability
	0	$x_0(A, B) = \frac{1}{Z}$
	1	$x_1(A, B) = \frac{A}{K_A Z}$
	2	$x_2(A, B) = \frac{B}{K_B Z}$
	3	$x_3(A, B) = \frac{AB}{K'_A K_B Z}$

Fig. 2. Gene states. As an illustration consider two transcription factors,  $A$  and  $B$ , which can each bind to a specific regulatory site. Accordingly, four states can be distinguished. The probabilities to find these states depend on the concentrations  $A$  and  $B$  as shown, where  $K_A$  and  $K_B$  denote the dissociation constants of the factors from their sites, when the other factor is not present.  $K'_A$  is the dissociation constant for  $A$  when  $B$  is already bound, which can account for cooperativity between  $A$  and  $B$ .  $Z = 1 + A/K_A + B/K_B + (AB)/(K'_A K_B)$ . In the mathematical model, the probabilities are used to calculate the rate of transcription.

where we have denoted the free concentrations of the various binding factors by  $F_1, F_2, \dots, F_N$ .  $\Delta G_{0,s}$  is the standard free energy difference between state  $s$  and the empty promoter evaluated for the reference concentrations of free ligand  $F_{i,0}$ . Observing that the probabilities over all possible states sum to unity, this expression can be rearranged to find the probability of state  $s$ :

$$x_s(F_1, \dots, F_N) = \gamma_s / \sum_{r=0}^S \gamma_r. \quad (2.4)$$

A simple example of such an evaluation is provided in Fig. 2. The free energy differences  $\Delta G_{0,s}$  are related to the measurable dissociation constants of the ligands from their binding sites. In the case that all transcription factors bind independently of one another, which may be justifiable as an approximation, the state probabilities take the simpler form

$$x_s(F_1, \dots, F_{m+n}) = \underbrace{\prod_{i=1}^m \frac{F_i}{K_i + F_i}}_{\text{bound factors}} \underbrace{\prod_{i=m+1}^{m+n} \frac{K_i}{K_i + F_i}}_{\text{unbound factors}}. \quad (2.5)$$

However, in many cases, cooperativity of binding is observed. If the cooperativity is very pronounced, the state probabilities may be simplified again. For example, if we assume for the system shown in Fig. 2 that binding of the regulator  $A$  is greatly enhanced if regulator  $B$  is already present at its site (and vice versa), such that  $K'_A \ll K_A$  and  $K'_B \ll K_B$ , the probability of the fully occupied state is approximately

$$x_3 \approx \frac{AB}{K'_A K_B + AB}, \quad (2.6)$$

which in the special case of a tandem site for the same factor (i.e.,  $A$  and  $B$  are identical molecules) gives the familiar Hill expression  $x_3 \approx A^2/(K^2 + A^2)$ , where

$$K = \sqrt{K_A K'_A}.$$

A quantitative determination of the state probabilities  $x_s$  from experimental data has been carried out for the  $\lambda$ -phage repressor (Ackers et al., 1982) and for the lac operon in *Eschericia coli* (Setty et al., 2003). The rates  $v_s$  at which transcription proceeds from the configurations  $s$  need to be supplied as parameters to the model, and may be estimated from data (Setty et al., 2003).

To complete model (2.1), the rates of translation, and mRNA and protein degradation need to be specified. For ease of mathematical notation, we will abbreviate the concentrations of mRNA and protein:  $R = [\text{mRNA}]$ ,  $P = [\text{protein}]$ . In a first approximation, we can use first-order kinetics for the remaining rates

$$v_{\text{translation}} = k_T R, \quad v_{\text{mRNA degradation}} = k_R R, \quad v_{\text{protein degradation}} = k_P P, \quad (2.7)$$

where  $k_T$ ,  $k_R$  and  $k_P$  are the rate constants of translation, mRNA degradation, and protein degradation, respectively. Having thus introduced the kinetic equations that describe gene expression, we turn to the analysis of simple gene regulatory networks.

## 2.2. Qualitative behavior and bifurcations in regulatory networks

Prototypical cases of regulation arise when the gene product is a transcription factor that regulates transcription of its own gene. A number of gene regulatory loops have been identified in which a protein either inhibits or activates transcription of its gene, and below we refer to examples in eukaryotic cells. An excellent review focusing on recent work on prokaryotic gene regulation has been provided by [Hasty et al. \(2001\)](#). In this section, we outline the methods of model analysis and their results for such feedback loops. In Section 3, we study in detail the regulation of the autoactivating zinc finger protein GATA-3, for which recently many experimental data have become available.

### 2.2.1. Autoinhibition

To be specific, let the protein bind to  $n$  regulatory sites in its gene at which it inhibits transcription. For mathematical simplicity, we assume that transcription only takes place when no inhibitor is bound, so that we obtain

$$\frac{dR}{dt} = v_{\max} \left( \frac{K_P}{K_P + P} \right)^n - k_R R, \quad \frac{dP}{dt} = k_T R - k_P P, \quad (2.8)$$

where the inhibitor molecules are taken to bind independently to each individual site with dissociation constant  $K_P$ . However, more complicated mechanisms, for which the extent of inhibition depends on the number and position of bound inhibitors may also be described. In general, additional factors will be necessary for transcription. These can be considered as control parameters that determine the value of the maximal transcription rate  $v_{\max}$ . External signals may control some of these factors through signal transduction pathways. An example of such regulation, where external IL-4 stimulates, in a time-dependent manner, the transcription of GATA-3 through the Stat6 pathway, is provided in Section 3. Solutions for the nonlinear differential equation system (2.8) are not available in closed form. However, the system behavior can be deduced by stability analysis and numerical simulations.

The steady states, in which neither mRNA nor protein concentrations change, are found by setting  $dR/dt = dP/dt = 0$ . This yields the implicit equation for the steady-state protein concentration  $\bar{P}$ :

$$\frac{v_{\max} k_T}{k_R} \left( \frac{K_P}{K_P + \bar{P}} \right)^n = k_P \bar{P}, \quad (2.9)$$

the solutions of which can be visualized as the intersection points of the two functions of  $\bar{P}$  defined by the left-hand side—the protein production rate, and the right-hand side—the protein degradation rate. As seen in [Fig. 3A](#), there is a unique steady state. More detailed analysis shows that this steady state is stable with respect to random perturbations.

To investigate stability, we assume that the steady states in mRNA and protein concentration,  $\bar{R}$  and  $\bar{P}$ , respectively, are changed by quantities  $r(t)$  and  $p(t)$  which reflect inevitably present random perturbations. If  $r(t)$  and  $p(t)$  are small compared with  $\bar{R}$  and  $\bar{P}$ , their time evolution is given by a linear system

$$\frac{dr}{dt} = ap + br, \quad \frac{dp}{dt} = cp + dr, \quad (2.10)$$

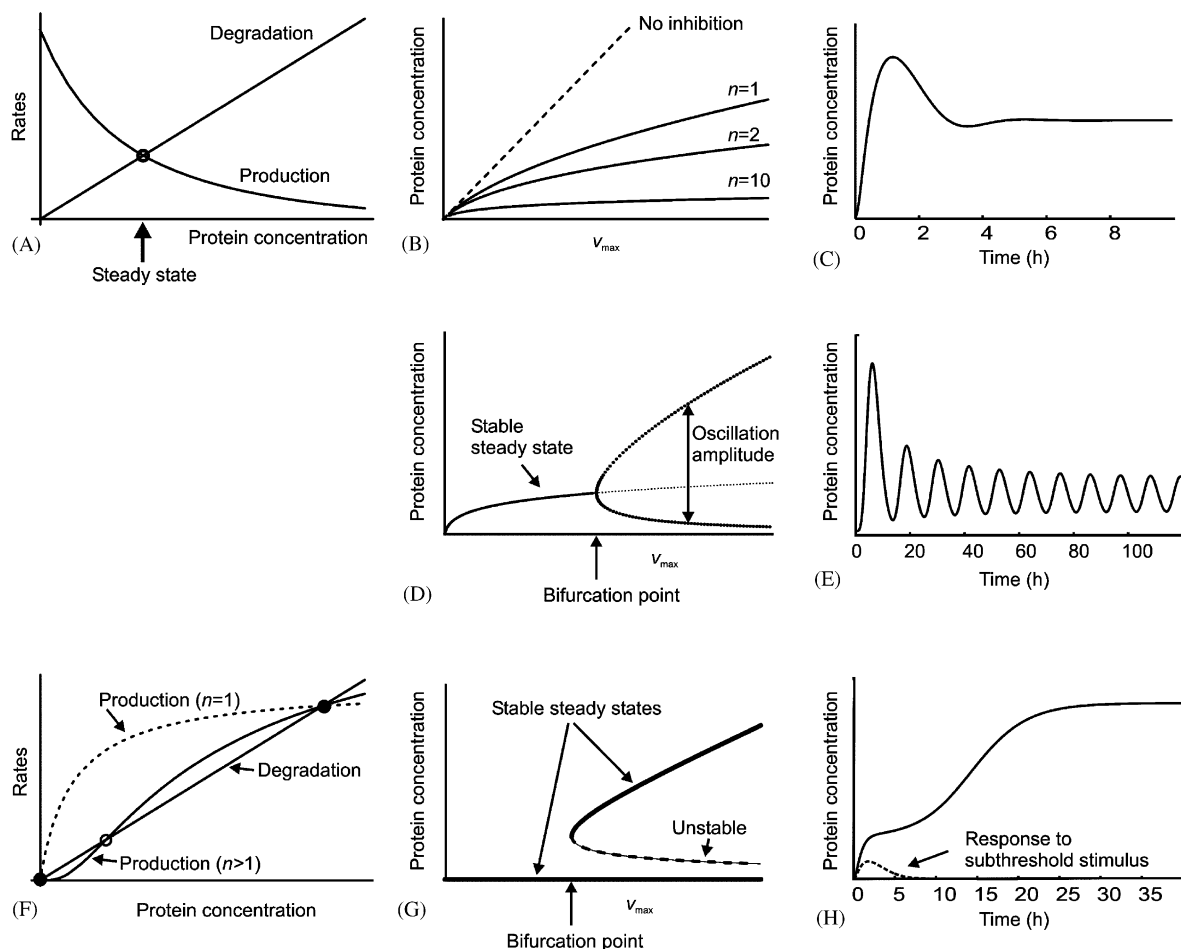


Fig. 3. Behavior of simple gene-regulatory loops. (A) The expression dynamics of protein acting as an autorepressor admits a unique steady state when production and degradation rates balance (circle). (B) When the maximal expression rate  $v_{\max}$  is increased (e.g., by increasing the nuclear concentration of an activator of the gene), autoinhibition is seen to prevent a strong increase in the steady-state concentration of the protein. This homeostatic effect is the stronger the more sigmoid the autoinhibition response is (as measured by the Hill coefficient  $n$ ). (C) A temporal response of the system to an increase in  $v_{\max}$  shows an initial overshoot before autoinhibition takes effect. (D) When the delay from transcription start to the appearance of active autorepressor in the nucleus becomes too long, the steady state becomes unstable at a critical value of  $v_{\max}$  (Hopf bifurcation point) and self-sustained oscillations in the concentrations of mRNA and protein develop. (E) Time course of protein oscillations. (F) The expression dynamics of protein acting as an autoactivator admit either two steady states, one of which is stable (monostability), or three steady states, two of which are stable (bistability). When the autoactivation response is hyperbolic (Hill coefficient  $n = 1$ , dashed line) the system is always monostable. In contrast, a sigmoid autoactivation response, as it would be generated by multiple binding sites for the autoactivator, can result in bistability (solid line; filled circles: stable states; open circle: unstable state). (G) Similar to the case of oscillations shown in Fig. 3D, bistability arises at a critical value of  $v_{\max}$  (a saddle-node bifurcation point). (H) When  $v_{\max}$  is larger than this bifurcation value, a sufficiently large external stimulus can push the mRNA and protein concentrations permanently into the high-expression steady state (solid line, shown only for protein). However, if the external stimulus is too weak, gene expression is transient and returns to the off-state (dashed line). The stimulus was modeled as an initial increase in mRNA concentration, which could be caused by transient activation of a signaling pathway (for details see Section 3).

where we have specifically

$$a = -\frac{nv_{\max}K_P^n}{(K_P + \bar{P})^{n+1}}, \quad b = -k_R, \quad c = k_T, \quad d = -k_P. \quad (2.11)$$

Linear differential equation systems such as Eq. (2.10) have either exponentially growing solutions, in which case the steady state is unstable, or solutions decaying exponentially to zero, which imply that the steady state is asymptotically stable. It can be shown that all perturbations decay, and hence the steady state is stable, if, and only if,

$$a + b < 0 \quad \text{and} \quad ad - bc > 0. \quad (2.12)$$

It is easily verified that inequalities (2.12) are satisfied for any values of the kinetic parameters and therefore the steady state is stable. The same type of analysis can be carried out when the kinetic equations involve more than two variables. A general condition for establishing stability, comparable to (2.12), exists (Hurwitz criterion; for a more detailed exposition of stability analysis see, e.g., Strogatz, 1994; and for applications to biochemical systems Heinrich et al., 1977; Heinrich and Schuster, 1996).

To evaluate how gene expression is controlled by autoinhibition, we consider the situation that transcription is initially switched off due to the unavailability of an activating factor ( $v_{\max} = 0$ ), and that this factor becomes present and hence  $v_{\max} > 0$ . A steady state of transcription will be achieved, in which autoinhibition has an expected homeostatic effect on the steady-state protein concentration (Fig. 3B). The more inhibitory sites are present, the less responsive the steady-state protein level becomes to the maximal transcription rate (Fig. 3B, compare the stimulus–response curves without inhibition—dashed line—and for 2, and 10 sites—solid lines as labeled).

In time, an initial overshoot in the approach to the steady state may be observed (Fig. 3C). During the initial phase of transcription no protein is present for autoinhibition, and only after protein has been produced in sufficient quantity, inhibition sets in. Therefore the delay between transcription and protein synthesis is crucial for the temporal behavior of the autoinhibition loop. This dependence of the dynamics on the delay in protein synthesis has a striking consequence when the feedback delay becomes larger. This is realized when there are more than two steps in the regulatory loop. Assuming, for example, that the protein requires phosphorylation to exert its inhibitory action, system (2.8) is extended to

$$\frac{dR}{dt} = v_{\max} \left( \frac{K_P}{K_P + P^*} \right)^n - k_R R, \quad \frac{dP}{dt} = k_T R - (k_K + k_P) P, \quad \frac{dP^*}{dt} = k_K P - k_{P^*} P^*, \quad (2.13)$$

where  $P^*$  is the concentration of the phosphorylated form and  $k_K$  is the rate constant of the protein kinase. (Note that  $P^*$  could also stand for a second protein that is stimulated to act as a transcriptional inhibitor by  $P$ . Thus the negative feedback could be conveyed through a signaling chain.) Analysis carried out in a similar fashion as shown above yields a unique steady state for each value of the maximal transcription rate. However, the stability of the steady state is no longer guaranteed. The steady state is found to be stable for low maximal transcription rate  $v_{\max}$  (Fig. 3D, solid line; compare with 3B) but becomes unstable when  $v_{\max}$  exceeds a critical value (Fig. 3D, thin dotted line). The unstable state cannot be approached by the dynamics of the system, and, instead, *self-sustained oscillations* in mRNA and protein concentration set in

(Fig. 3D, thick dotted line, showing minima and maxima of oscillation as a function of  $v_{\max}$ ; Fig. 3E, showing the time course for a particular  $v_{\max}$ ).

Fundamental changes in the behavior of a system as a control parameter is varied, such as the onset of oscillations when  $v_{\max}$  is increased, are referred to as bifurcations. The type of bifurcation leading from the stable steady state to stable oscillations is a Hopf bifurcation (see Strogatz, 1994; Goldbeter, 1996). Theoretical analyses carried out on negative feedback systems in transcriptional control show that such systems can behave in an oscillatory fashion if the feedback delay is sufficiently long (Goodwin, 1963; Hunding, 1974; Tyson and Othmer, 1978). Many processes can contribute delays, including RNA and protein synthesis (see Monk, 2003), RNA processing and nuclear export, and protein modifications and nuclear import.

The conditions for negative feedback oscillations in gene expression could thus be readily met in cells. Recently, such oscillations have been observed in several eukaryotic systems, involving the expression of p53 (Bar-Or et al., 2000), NF $\kappa$ B (Hoffmann et al., 2002), and Hes1 (Hirate et al., 2002). Regular transcriptional oscillations could be employed as timekeeping mechanisms. Indeed, there is strong evidence that circadian oscillators rely on autoinhibition circuits in the expression of key transcription factors (e.g., Goldbeter, 1996). Similar timing mechanisms may be at work in segmentation during vertebrate development (Lewis, 2003).

### 2.2.2. Autoactivation

We assume that the protein activates the transcription of its gene when bound to  $n$  regulatory sites. Thus we obtain

$$\frac{dR}{dt} = v_{\max} \left( \frac{P}{K_P + P} \right)^n - k_R R, \quad \frac{dP}{dt} = k_T R - k_P P. \quad (2.14)$$

A steady state is again obtained when the protein synthesis rate and degradation rate balance:

$$\frac{v_{\max} k_T}{k_R} \left( \frac{\bar{P}}{K_P + \bar{P}} \right)^n = k_P \bar{P}. \quad (2.15)$$

In this particular system,  $R = 0$  and  $P = 0$  is always a steady state, because in Eq. (2.14) autoactivation is strictly required for expression. Whether this state is stable or not depends on the slope of the synthesis function (left-hand side of Eq. (2.15)) compared with the slope of the degradation function (right-hand side of Eq. (2.15)) at  $P = 0$ . If synthesis increases hyperbolically with protein concentration (Fig. 3F, dashed curve), which is the case when there is only one activator binding site, then the zero state is unstable. In this case, there is another steady state with non-zero protein expression, which is stable and therefore assumed by the system (Fig. 3F).

The system behavior is qualitatively different when the autoactivation response is sigmoid, which will result from the presence of more than one binding site (Fig. 3F, sigmoid solid curve). Then three steady states can occur of which the outer two are stable (Fig. 3F, filled circles) and the middle state is unstable (Fig. 3F, open circle). Therefore the system has access to two steady states at once—a phenomenon referred to as *bistability*. Which state will be attained is determined by the initial conditions. We can again consider the maximal transcription rate  $v_{\max}$  as a control parameter whose value is set by the availability of additional activators (Fig. 3G). For low values of  $v_{\max}$  there is only one steady state, which is the zero state. At a bifurcation point, two new steady states—a stable and an unstable one—arise. Therefore the system exhibits an inherent

threshold, and sustained transcription can only occur when  $v_{\max}$  exceeds this threshold. However, note that an increase in  $v_{\max}$  alone cannot affect a transition from the zero state to sustained expression in this system, because the zero state is always stable. To achieve this, one requires an additional activation of transcription that is independent of autoactivation and can be transient. If such an external impulse is sufficiently large, the expression of the gene will be switched on (Fig. 3H).

### 2.2.3. Cross-inhibition

Bistability and thresholds can also arise from inhibitory regulatory interactions if they are appropriately coupled. A network of this kind consists of a pair of mutually inhibitory transcription factors (Fig. 4A). Intuitively, one can expect two alternative steady states in which one of the factors is highly expressed and inhibits the other one. The corresponding kinetic model reads

$$\frac{dR_1}{dt} = v_{\max,1} \left( \frac{K_2}{K_2 + P_2} \right)^{n_2} - k_{R,1}R_1, \quad \frac{dP_1}{dt} = k_{T,1}R_1 - k_{P,1}P_1, \quad (2.16)$$

$$\frac{dR_2}{dt} = v_{\max,2} \left( \frac{K_1}{K_1 + P_1} \right)^{n_1} - k_{R,2}R_2, \quad \frac{dP_2}{dt} = k_{T,2}R_2 - k_{P,2}P_2, \quad (2.17)$$

where the mRNA and protein concentrations of the two species are distinguished by the indices 1 and 2.  $K_1$  and  $K_2$  are the dissociation constants of protein 1 and 2 for the regulatory sites in genes 2 and 1, respectively. Although now there are two interacting proteins, the steady-state analysis

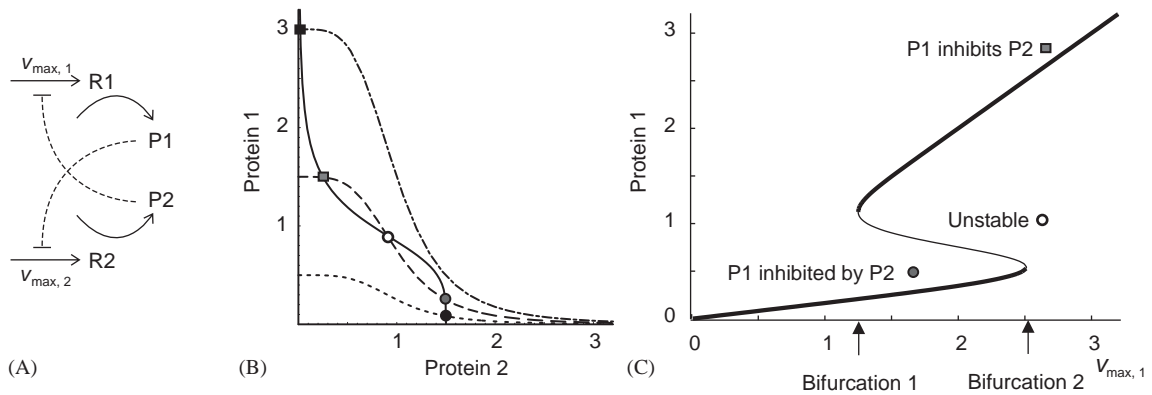


Fig. 4. Behavior of a network of two mutually repressive genes. (A) Protein 2 (P2) inhibits transcription of protein 1 (P1) and vice versa. (B) Given a certain level of P2, we can calculate the steady state of P1, which clearly is a decreasing function of its repressor P2 (dotted, dashed and dot-dashed lines, calculated for increasing maximal transcription rates of P1,  $v_{\max,1}$ ). The corresponding steady-state curve for P2 versus its repressor P1 has the same shape (solid line; note that for this curve the P1 axis plays the role of the abscissa). The system is at steady state, when both P1 and P2 are, which is the case at the intersection points. Detailed analysis shows that there can be either one or two stable intersection points (filled symbols); the intersection marked by the open circle is always unstable. (C) As  $v_{\max,1}$  is increased, the system switches from a state in which P1 is repressed by P2 (filled circles in Fig. 4B) to a state in which P1 represses P2 (filled squares in Fig. 4B) at bifurcation point 2. When  $v_{\max,1}$  is decreased, the reverse switch takes place at bifurcation point 1. This history dependence of switching is referred to as hysteresis.

can be conducted in a similar geometric manner as for one protein. The steady-state protein concentrations,  $\bar{P}_1$  and  $\bar{P}_2$ , are given by the coupled equations

$$\bar{P}_1 = \frac{v_{\max,1}k_{T,1}}{k_{P,1}k_{R,1}} \left( \frac{K_2}{K_2 + \bar{P}_2} \right)^{n_2}, \quad \bar{P}_2 = \frac{v_{\max,2}k_{T,2}}{k_{P,2}k_{R,2}} \left( \frac{K_1}{K_1 + \bar{P}_1} \right)^{n_1}. \quad (2.18)$$

The first of these can be plotted as a function  $\bar{P}_1$  versus  $\bar{P}_2$ , the second as a function  $\bar{P}_2$  versus  $\bar{P}_1$ . Hence in the  $\bar{P}_1 - \bar{P}_2$  plane, one obtains two lines, the intersections of which are the steady states. In Fig. 4B, the maximal transcription rate of protein 1,  $v_{\max,1}$ , was considered as control parameter: the solid line corresponds to unchanging  $\bar{P}_2$ , while the broken lines correspond to unchanging  $\bar{P}_1$  for different values of  $v_{\max,1}$ . At low transcription rate of protein 1,  $v_{\max,1}$ , (short dashed line), there is one steady state in which high  $P_2$  suppresses expression of  $P_1$  (black circle). As  $v_{\max,1}$  is increased, two further states arise, one being stable (gray square), the other unstable (open circle). Thus there is now a bistable situation in which either  $P_2$  suppresses  $P_1$  (gray circle) or vice versa (gray square). When  $v_{\max,1}$  becomes even higher (dot-dashed line), the bistability disappears again and  $P_1$  becomes dominant (black square). The steady-state  $\bar{P}_1$  traces the curve shown in Fig. 4C as  $v_{\max,1}$  is varied. Note that when  $v_{\max,1}$  is increased, an abrupt transition occurs at bifurcation point 2, while when  $v_{\max,1}$  is decreased the transition occurs at bifurcation point 1—a phenomenon known as hysteresis.

#### 2.2.4. Threshold responses

We have seen that in both paradigm models exhibiting bistability—autoactivation and cross-inhibition—sufficiently steep sigmoid responses of the transcription rate to activator or inhibitor concentrations are required. As has been discussed, sigmoidicity arises naturally when the regulator must bind to several sites at once, and sigmoidicity is steepened when the binding is cooperative. However, an additional, or alternative, source of sigmoidicity could be multiple phosphorylation in the regulation of transcription factor activity (Salazar and Höfer, 2003; Markevic et al., 2004; Xiong and Ferrell, 2004). Moreover, when a regulator affects several steps of the sequential assembly of the basic transcription machinery (see Cosma, 2002), e.g., by influencing the state of chromatin at the promoter, a sigmoid response curve with respect to regulator concentration can result (Rasch and Höfer, submitted).

### 2.3. Stochastic description of gene expression

So far, we have treated gene regulation as a deterministic process in the sense that, given the knowledge on the regulatory elements of the gene and the concentrations of the regulators, the transcription rate is determined. However, the binding and dissociation of the regulators will be affected by molecular fluctuations, and therefore the state of each individual gene copy will change in a randomly fluctuating manner. As most genes only exist in one or two copies per cell, the fluctuations may become manifest at mRNA and protein levels. To include such molecular noise in a description of gene regulation, we consider the simple scheme of transcription initiation depicted in Fig. 5A (Rasch and Höfer, submitted). It consists of two steps: the binding of an activator that recruits RNA polymerase to the promoter, and the binding of RNA polymerase that may initiate transcription or dissociate again (Fig. 5A). For simplicity, we only account for mRNA synthesis.

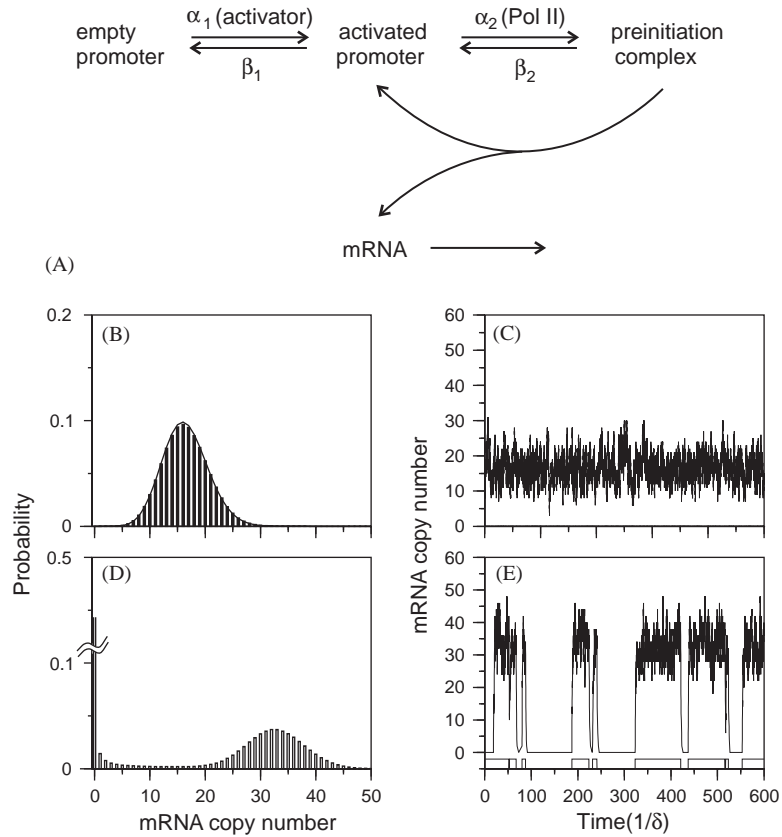


Fig. 5. Stochastic model of transcription initiation. (A) Binding of an activator precedes the recruitment of RNA polymerase II (Pol II); the respective binding and dissociation rate constants are denoted by  $\alpha_1$ ,  $\alpha_2$ ,  $\beta_1$  and  $\beta_2$ . Pol II initiates transcription with rate  $\theta$ , and mRNA is degraded with rate constant  $\delta$ . (B) When exchange of activator and Pol II are much faster than the two subsequent steps, a unimodal mRNA distribution results, for which the mean value can also be correctly predicted by a deterministic model. (C) Sample time course of mRNA fluctuations in a cell corresponding to Fig. 5B (the time units are mRNA half lives). (D) When the initial step of activation is very slow, however, bimodal mRNA distributions can be obtained, and (E) transcription in a single cell viewed over many mRNA half-lives is burst-like. Analysis shows that this is a rather extreme case which would occur when the time scale of the initial steps in transcription initiation (measured by  $\alpha_1$  and  $\beta_1$ ) is much slower than the mRNA half-life.

A stochastic description of this scheme considers the probability that the gene is in state  $s$  and that there are  $m$  mRNA molecules:  $W(s, m)$ . The time evolution of  $W(s, m)$  is given by the master equation that balances the processes by which a particular state  $(s, m)$  can be reached and left. It is of the general form

$$\frac{d}{dt} W(s, m) = \underbrace{\alpha_{s-1} W(s-1, m) + \beta_{s+1} W(s+1, m)}_{\text{change of gene state}} - (\alpha_s + \beta_s) W(s, m)$$

$$\begin{aligned}
& + \underbrace{\theta_s(W(s, m-1) - W(s, m))}_{\text{mRNA synthesis}} \\
& + \underbrace{\delta[(m+1)W(s, m+1) - mW(s, m)]}_{\text{mRNA degradation}}, \tag{2.19}
\end{aligned}$$

forming a system of differential equations for the various promoter states  $0 \leq s \leq s_{\max}$  and mRNA copy numbers  $m \geq 0$ . The parameters  $\alpha_s$  and  $\beta_s$  denote the first-order binding and dissociation rate constants of transcription factors to the gene;  $\theta_s$  and  $\delta$  and are the rate constants of transcription initiation from the gene in state  $s$  and of mRNA degradation, respectively. The analysis of master equations is rather complicated and, in general, analytical results cannot be expected. However, in the special case that the transitions between the gene states are much faster than mRNA synthesis and degradation, one can show for the scheme of Fig. 5A that transcription proceeds with an effective rate

$$\theta' = \frac{\theta}{1 + \frac{E}{K_E} \left(1 + \frac{A}{K_A}\right)}, \tag{2.20}$$

where  $A$  and  $E$  denote the concentrations of activator and RNA polymerase, respectively, and  $K_A$  and  $K_E$  are the respective dissociation constants. The steady-state probability of mRNA molecules in the cell obeys the Poisson distribution

$$W(m) = \frac{1}{m!} \left(\frac{\theta'}{\delta}\right)^m e^{-\theta'/\delta}. \tag{2.21}$$

The mean value,  $\bar{m}$  and variance  $\sigma^2$  of this distribution are both equal to  $\theta'/\delta$ , which implies that the relative size of mRNA fluctuations, given by the coefficient of variation, is

$$CV = \frac{\bar{m}}{\sigma} = \frac{1}{\sqrt{\bar{m}}}. \tag{2.22}$$

The fluctuation size decreases with increasing average mRNA copy number with the inverse square-root law known from fluctuations in many physical and chemical systems. This result shows that the deterministic approach taken above is valid, when the transitions between the gene states are fast and the mRNA copy number is sufficiently large. The mRNA distribution shown as an example in Fig. 5B has an average of 15 copies; a sample time course shows mRNA fluctuations on the time scale of the mean mRNA lifetime (Fig. 5C). It should be noted that the deterministic approach in this case will yield the correct average mRNA number (and the fluctuation size can be found according to Eq. (2.22)). Thus a crucial assumption for the applicability of the deterministic description is that gene state transitions are rapid processes, such that mRNA synthesis and degradation will average over the molecular fluctuations in promoter states. This may often hold, especially, when the transitions are based solely on binding and dissociation of transcription factors (Dundr et al., 2002; Kimura et al., 2002).

If this separation of time scales does not hold, the deterministic description will generally fail to describe the dynamics accurately. The most pronounced case of such failure occurs when initial steps in transcription initiation are very slow (in the scheme in Fig. 5A, this is the case when  $\alpha_1$  and  $\beta_1$  are about an order of magnitude smaller than the mRNA degradation rate constant  $\delta$ , while  $\alpha_2$  and  $\beta_2$  are of the order of  $\delta$  or larger). Then the mRNA probability can become bimodal

(Fig. 5D): when the initial steps have not occurred, there is no transcription at all (left peak); after they have occurred, repetitive transcription initiation results in a high mRNA level (right peak). Viewed over many mRNA half lives, transcription dynamics are then burst-like (Fig. 5E). Bimodal mRNA distribution and bursting kinetics arise due to the relay of the slow activator exchange fluctuations to transcription. Therefore this behavior can be captured by a stochastic model but not by a deterministic description. Interestingly, stochastic behaviour can be observed in cytokine expression by T cells (e.g. Hu-Li et al., 2001).

### 3. Transcriptional control networks in helper T cell differentiation

#### 3.1. The autoactivation switch of the transcription factor GATA-3

Autoactivating transcription factors like myo-D, Pit-1, GATA-1 and GATA-3 have been implicated as master regulators of cell differentiation (Tsai et al., 1991; Rhodes et al., 1993; Lun et al., 1997; Arnold and Winter, 1998; Ouyang et al., 2000). In recent years, experimental work has begun to uncover the molecular mechanisms for the regulation of GATA-3 in Th lymphocytes (reviewed in Löhning et al., 2002; Murphy and Reiner, 2002). This has allowed the formulation of a mathematical model based on the following assumptions (Fig. 6; see also Höfer et al., 2002):

- GATA-3 is expressed at a basal rate in naïve Th cells.
- GATA-3 expression is augmented by activation of Stat6, which occurs through external IL-4. The effect of Stat6 is observed only with simultaneous TCR activation.
- GATA-3 increases its own expression.
- Both Stat6 and GATA-3 act independently on GATA-3 transcription.
- Autoactivation of GATA-3 exhibits a sigmoid response curve.

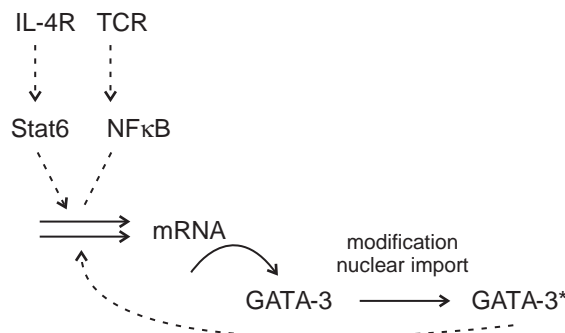


Fig. 6. Regulation of GATA-3 in Th cells. Transcription of GATA-3 can be stimulated independently by the IL-4/Stat6 pathway (Kurata et al., 1999), probably in cooperation with T cell receptor (TCR) controlled transcription factors such as NFκB (Das et al., 2001), and by GATA-3 autoactivation (Ouyang et al., 2000). Independent activation by two pathways could be related to the existence of two GATA-3 promoters (Asnagli et al., 2002). Posttranslational control steps of GATA-3 such as phosphorylation (Chen et al., 2000) and acetylation (Yamagata et al., 2000) have been described, and remain to be elucidated in more detail.

The first four statements follow from experimental results (Zheng and Flavell, 1997; Zhang et al., 1997; Ouyang et al., 1998; Kurata et al., 1999; Ouyang et al., 2000). That GATA-3 and activated Stat6 directly stimulate GATA-3 transcription has not been shown explicitly; however, as they affect GATA-3 mRNA levels and are known to be transcriptional regulators, this is very likely. The fifth assumption has not been verified experimentally. However, regulatory sites for GATA transcription factors have been found to occur as doublets or triplets in cytokine genes (Siegel et al., 1995; Lavenu-Bombled et al., 2002; Radbruch et al., 2002). If a GATA tandem site were responsible for autoactivation of the GATA-3 gene (George et al., 1994; Gregoire and Romeo, 1999), a sigmoid response curve would be obtained. However, as indicated in the previous section, sigmoid response curves could also be generated by mechanisms other than multiple regulatory binding sites.

To formulate these assumptions mathematically, we denote the GATA-3 transcription rates achieved under the different conditions as follows: basal— $v_B$ ; Stat6-induced— $v_{\max,S}$ ; GATA-3-induced— $v_{\max,G}$ . For simplicity, we assume that when both GATA-3 and activated Stat6 are present the rate is  $v_{\max,S} + v_{\max,G}$ . Then the balance equations for the GATA-3 mRNA and protein concentrations,  $R$  and  $G$ , respectively, read:

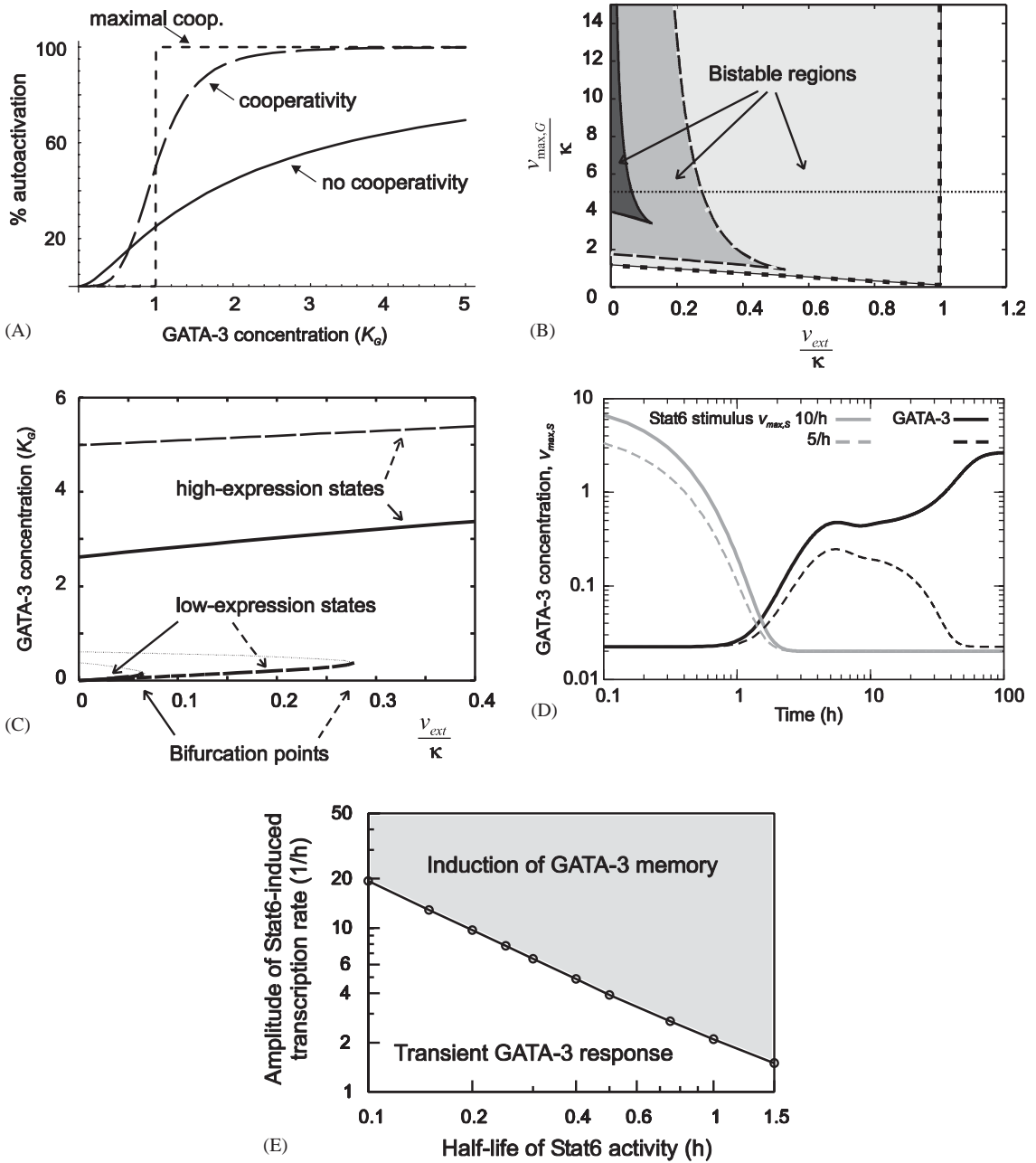
$$\frac{dR}{dt} = v_B + v_{\max,S} \frac{S}{K_S + S} + v_{\max,G} \left( \frac{G}{K_G + G} \right)^2 - k_R R, \quad \frac{dG}{dt} = k_T R - k_G G, \quad (3.1)$$

where  $G$  and  $S$  denote the nuclear concentrations of GATA-3 and active Stat6.  $K_S$  and  $K_G$  are the dissociation constants of an active Stat6 dimer and of GATA-3 at their respective regulatory sites. The autoactivation rate in Eq. (3.1) assumes the independent binding of two GATA-3 molecules to a tandem site (Fig 7A, solid line). However, the binding may also be cooperative, and in the case of strong cooperativity, a steeper autoactivation response would be obtained (Fig. 7A, long-dashed line; see also Eq. (2.6)). As we do not know the actual cooperativity in the GATA-3 gene,

Fig. 7. The GATA-3 autoactivation switch. (A) Autoactivation of GATA-3 transcription as a function of GATA-3 protein concentration in the mathematical model. Two independent GATA sites result in a sigmoid response curve (solid line). The sigmoid response can be steepened by several GATA sites mediating cooperative binding of GATA-3 (long-dashed line, Hill kinetics with  $n = 4$ ). The maximal cooperativity that is theoretically conceivable (though probably not realizable) is indicated by the short-dashed line. (B) Sigmoid autoactivation causes bistability. Whether the system is bistable, depends on two parameters, determined by the Stat6-induced transcription rate ( $v_{\text{ext}}$ ) and on the GATA-3 autoactivation rate ( $v_{\max,G}$ ). The more pronounced the sigmoidicity of the autoactivation response, the larger the bistable region becomes (solid, long-dashed, and short-dashed lines correspond to the curves in Fig. 7A). When  $v_{\text{ext}}$  is varied along the dotted horizontal line, the stimulus response curves in (C) result (shown as in Figs 7A and B for independent binding to a tandem GATA site: solid line; and cooperativity with Hill coefficient four: long-dashed line). Two stable branches are recognizable in each case: one with low and another with high GATA-3 expression. Increasing the Stat6 signal beyond a threshold defined by the bifurcation point causes an irreversible switch from the low-expression to the high-expression branch. (D) Kinetics of the switch for transient Stat6 signals. If the amplitude of the Stat6 signal is sufficiently large ( $v_{\max,S} = 10/\text{h}$ ; gray line), GATA-3 can be switched from the low-expression state to the high-expression state (thick dashed and solid lines for mRNA and protein, respectively). The high-expression state sustains itself by autoactivation. In contrast, if the Stat6 stimulus is subcritical ( $v_{\max,S} = 5/\text{h}$ ), GATA-3 expression becomes only transiently activated (thin dashed and solid lines). Note that GATA-3 autoactivation requires the Stat6 stimulus to become active and cannot activate itself. (E) GATA-3 expression as a function of amplitude and duration of the Stat6 stimulus. The duration is taken as the half-life of an exponentially decaying Stat6 stimulus. For details of parameter values, see Höfer et al. (2002).

we also consider as a limiting case the steepest possible response, although this is unlikely to be realized by a biochemical mechanism (Fig. 7A, short-dashed line).

For the following considerations, we will combine the transcriptional regulation that is independent of autoactivation in a single term,  $v_{ext}$ , which contains the basal transcription rate



and the external control by the IL-4/IL-4R/Stat6 pathway:

$$v_{\text{ext}} = v_B + v_{\text{max},S} \frac{S}{K_S + S} \quad (3.2)$$

The system then has the same structure as Eq. (2.14), except for the additional term  $v_{\text{ext}}$ ; this term turns out to operate the autoactivation switch.

From the analysis in Section 2.2, we expect the GATA-3 system to exhibit bistability—implying that a state of low expression and a state of high expression are simultaneously available to the system. The analysis shows that there are two effective parameters that affect the steady state, which are combinations of the kinetic parameters in the model:  $v_{\text{ext}}/\kappa$  and  $v_{\text{max},G}/\kappa$ , where  $\kappa = k_R k_G / k_T$ . At present it is not known which values these parameters take in Th cells, or any other cell type. However, we can characterize the behavior of the system in the plane of all possible parameter values. The result of this computation yields a parameter region in which the system is bistable, which has the same principal shape for any sigmoid autoactivation response (Fig. 7B). The size of the bistable region is larger for steeper autoactivation responses.

To obtain bistability, the parameter  $v_{\text{max},G}/\kappa$ , measuring essentially the autoactivation rate, needs to exceed a critical value. Varying the externally controlled—through the IL-4/Stat6 pathway—transcription rate, a straight line in the parameter plane is traced (Fig. 7B, dotted line). Plotting the steady-state GATA-3 concentration along the straight line yields the response curve of the system to the external stimulus. It consists of two stable branches, with low and high GATA-3 expression, respectively (Fig. 7C, solid lines and long-dashed lines corresponding to the autoactivation kinetics marked likewise in Fig. 7A). Low GATA-3 expression is correlated with the naive Th cell state, while high expression is the hallmark of Th2-polarized cells. At a critical value of the external stimulus the low-expression branch disappears via a saddle-node bifurcation (Fig. 7C, bifurcation point). Therefore, when the external stimulus crosses this threshold, GATA-3 expression switches to the high-expression branch. As the high-expression branch always exists, the system will remain there even when the external stimulus disappears. Therefore a transient Stat6 stimulus (time course in Fig. 7D, solid gray line) can permanently switch on autoactivation (Fig. 7D, solid black line; note the slow evolution to the high-expression state shown on logarithmic time scale). However, if the amplitude of the transient Stat6 stimulus is too small (Fig. 7D, dashed gray line), GATA-3 elevation also remains transient and returns to the basal steady state (Fig. 7D, dashed black line). In fact, both amplitude and duration of the Stat6 signal jointly determine the outcome of the stimulus. To achieve GATA-3 memory expression, a small amplitude of the Stat6 signal can be compensated for by a sufficiently long duration or vice versa. This is illustrated in Fig. 7E which shows, for a continuous gradation of Stat6 stimuli, the resulting GATA-3 expression, being transient below the critical line (Fig. 7E, white area) and permanent above it (Fig. 7E, gray area). Thus the GATA-3 autoactivation loop converts graded Stat6 activities in a binary transcriptional response.

The capacity of a transient signal to switch on GATA-3 expression irreversibly is connected with the incomplete hysteresis loop shown in Fig. 7C. A complete hysteresis structure, as depicted in Fig. 4C, could not serve the same function, because the protein expression level would return to the low steady-state branch in the absence of continued stimulation. Irreversible transitions similar to the one described for GATA-3 expression have also been found in energy metabolism (Schellenberger and Hervagault, 1991).

To summarize, the regulation of GATA-3 expression gives rise to a sharp threshold for the external stimulus delivered through the IL-4/Stat6 pathway. Once the threshold is exceeded, the system switches to sustained high expression. The existence of an intrinsic activation threshold in the GATA-3 system is strongly supported by the observation that (transient) ectopic GATA-3 expression alone causes a dramatic and sustained increase in the expression of the endogenous GATA-3 gene (Ouyang et al., 2000).

### 3.2. Regulation of the GATA-3 autoactivation switch by inhibitors

Experimental results have indicated that the properties of the GATA-3 autoactivation switch can be regulated by inhibitors of GATA-3, such as FOG-1 (Zhou et al., 2001; Kurata et al., 2002) and ROG (Miaw et al., 2000). To date, however, it has not been elucidated how these inhibitors function. For FOG-1 it has been shown that it associates with GATA transcription factors (Tsang et al., 1997), while DNA binding has so far not been reported. This may suggest that FOG-1 forms a complex with GATA-3 in such a way that GATA-3 can no longer activate transcription or that a transcriptional repressor is recruited. ROG also associates with GATA-3 and prevents GATA-3 from binding DNA (Miaw et al., 2000). However, inhibitors could also repress GATA-3 transcription by binding to the DNA, thus interfering with basal transcription, Stat6-induced transcription, or GATA-3 autoactivation, or any combination of those. Therefore, we have studied three mechanisms for inhibition in the model: (i) the repressor associates with free GATA-3 molecules and prevents them from binding to DNA (in a similar fashion as described for inhibition of nuclear entry of NF $\kappa$ B by I $\kappa$ B; Fig. 8,  $R_1$ ); (ii) the repressor binds to DNA where it inhibits basal and Stat6-induced GATA-3 expression (Fig. 8,  $R_2$ ), and (iii) it binds to DNA inhibiting GATA-3 autoactivation (Fig. 8,  $R_3$ ). For details of the incorporation of the repressors in the model see Appendix A.

#### 3.2.1. Repressor sequesters free GATA-3

The behavior of the system crucially depends on whether only free GATA-3 is degraded or whether GATA-3 in the repressor complex can also be targeted for degradation. In the first case, the repressor can be shown to have no effect on the steady-state concentration of free, and thus transcriptionally active, GATA-3 protein. Intuitively, at steady-state synthesis and degradation

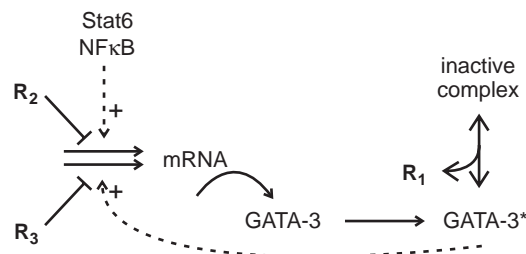


Fig. 8. Mechanisms for inhibition of GATA-3 expression studied in the model. Repressor 1 ( $R_1$ ) retains GATA-3 in an inactive complex (e.g., analogous to inhibition of NF $\kappa$ B by I $\kappa$ B; e.g., Hoffmann et al., 2002); repressor 2 ( $R_2$ ) interferes with basal and Stat6-induced transcription, whereas repressor 3 ( $R_3$ ) inhibits GATA-3 autoactivation.

rates balance, and if neither is affected by repressor-bound GATA-3, the steady-state is independent of the repressor concentration in the cell. The repressor simply acts as sponge that becomes soaked with GATA-3. If the repressor-bound GATA-3 can also be degraded, the repressor will cause a decrease in unbound, transcriptionally active GATA-3. As in this second case the impact of the repressor is very similar to a DNA-binding transcriptional repressor, which will be discussed in the following subsection, we only focus on the first case.

Although a GATA-3-sequestering repressor does not alter steady states of GATA-3 expression, it has a profound effect on the kinetics of transitions between the states. When GATA-3 levels rise, the repressor sequesters the protein, such that the rise in free, transcriptionally active, GATA-3 is delayed in a concentration-dependent manner (see Appendix A). When the system is subjected to a transient external stimulus, the inertia provided by the repressor can delay the switch to the GATA-3 high-expression state (Fig. 9A, for ratios of repressor concentration to its inhibition constant,  $I_{\text{tot}}/K_I$ , of 10 and 20), or, when the repressor concentration is sufficiently high, prevent the switch altogether (Fig. 9A;  $I_{\text{tot}}/K_I$  of 25 and 100; note that for  $I_{\text{tot}}/K_I = 25$  one can still notice a transient GATA-3 elevation due to the Stat6 stimulus). In contrast, when the system is already in the high-expression state and repressor is introduced (e.g., by transfection), it

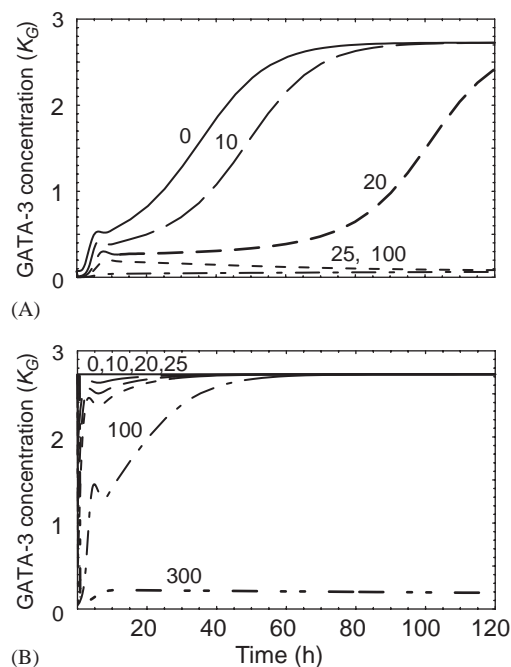


Fig. 9. Effect of a GATA-3 sequestering repressor on the autoactivation switch. (A) GATA-3 concentration after a supercritical Stat6 stimulus given in the GATA-3 low-expression state (cf. Fig. 7D). Simultaneous introduction of inhibitor— $R_1$  in Fig. 8—(with ratios of total inhibitor concentrations to dissociation constant of 10, 20, as indicated at the curves) delays the transition to the high-expression state but does not prevent it. Sufficiently high amounts of inhibitor (25, 100) prevent autoactivation. (B) By comparison, the GATA-3 high-expression state is more robust to the introduction of the inhibitor (the indicated inhibitor amount are given at once at  $t = 0$ ) and is abolished only at much higher inhibitor concentrations (300). For details of the models see Appendix A.

is much harder to suppress high GATA-3 expression (Fig. 9B). Immediately after addition of repressor, there is a drop in free GATA-3 protein concentration due to the binding to the repressor. However, over a large range of repressor concentrations, the system will recover the high-expression state (Fig. 9B). Remarkably, this behavior is similar to the observed effects of FOG-1 on GATA-3. Zhou et al. (2001) reported that IL-4/Stat6-induced GATA-3 induction is possible in the presence of FOG-1 overexpression but the switch to high GATA-3 expression is impaired. In already Th2-polarized cells, in which GATA-3 is highly expressed, FOG-1 overexpression seemed to have no inhibitory effect.

### 3.2.2. *Repression of basal GATA-3 transcription*

When basal transcription but not GATA-3 autoactivation is repressed, the repressor decreases the GATA-3 concentration in the low-expression state (Fig. 10A, line a). This will raise the threshold for IL-4/Stat6-induced switching to high GATA-3 expression. If in addition to basal transcription, Stat6-induced transcription is also repressed, the switch may be completely disabled. However, note that the high-expression state is practically unaffected by the repressor. When the system is in this state, it will remain there (Fig. 10A, line c). Thus the transcriptional repressor would appear very similar to a repressor sequestering GATA-3 in that it can inhibit or prevent the switching on of the autoactivation loop but would not abolish autoactivation once it is established. However, the model predicts different responses to retroviral transduction of an endogenous GATA-3 gene (see, e.g., Ouyang et al., 2000): a GATA-3 sponge can impair activation by this protocol (in a concentration-dependent manner), whereas the transcriptional repressor would be ineffective (data not shown).

Note that it is possible that the low-expression state does not exist without the repressor. This is the case when the basal transcription rate is sufficiently large (Fig. 10A, line b). Then the complete removal of the repressor, e.g., by degradation, actually triggers the autoactivation switch to sustained high GATA-3 expression. Interestingly, the GATA-3 inhibitor FOG-1 exhibits low-level expression in naïve Th cells and, after a transient rise during cell priming, is decreased in developed Th cells (Zhou et al., 2001; Kurata et al., 2002). This decrease, however, was seen both in Th1 and Th2 cells.

### 3.2.3. *Repression of GATA-3 autoactivation*

A repressor interfering with autoactivation would affect the high-expression state and have little impact on basal expression (Fig. 10B). Up to a critical value of repressor concentration, the high-expression level is decreased by the repressor and above the critical value ceases to exist altogether. Once the high-expression state has disappeared, IL-4/Stat6-induced transcription would result in a transient elevation of GATA-3 but could not trigger a switch to sustained expression.

## 3.3. *Conjectures on transcriptional cross-regulation of alternative cytokine memories*

Experimental data show that the main pathways of Th cell differentiation are regulated in a coordinated fashion. Cells can be primed to exhibit either Th1 or Th2 cytokine memory, associated with the elevation of either T-bet or GATA-3 (see Fig. 1). Stimuli that induce one differentiation pathway also suppress the other (Ouyang et al., 1998; Szabo et al., 2000). However,

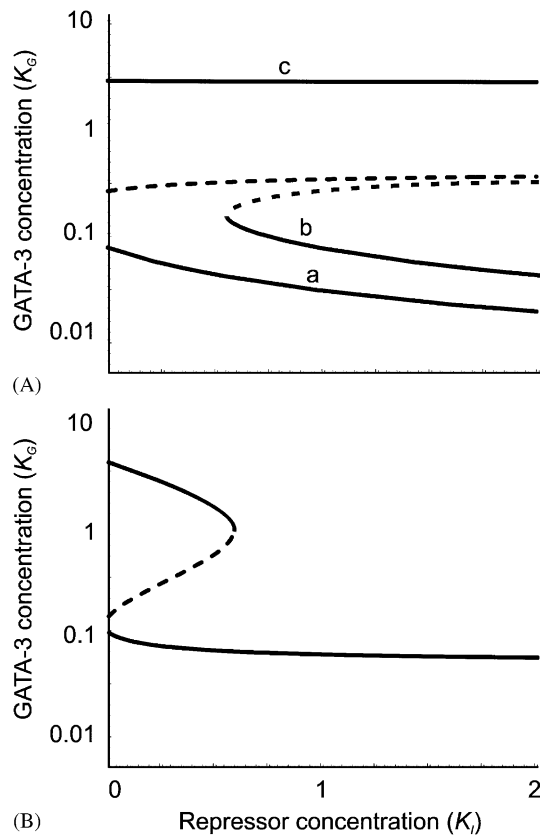


Fig. 10. Effects of transcriptional repression on the GATA-3 autoactivation switch. (A) A repressor acting on basal transcription ( $R_2$  in Fig. 8) decreases GATA-3 concentration in the low-expression state (branch a), while leaving the high-expression state practically unaffected (branch c). For different parameter values, it is possible that a certain repressor concentration is required for the low-expression state (branch b). (B) A repressor of GATA-3 autoactivation ( $R_3$  in Fig. 8) decreases the high-expression state, and, at sufficiently high repressor concentration, can cause it to disappear. It has little impact on basal GATA-3 expression. The GATA-3 expression model by Höfer et al. (2002) was used, augmented by repressor terms as described in Appendix A.

both Th1 and Th2 cytokine memories exhibit plasticity: short-term Th1-polarized cells can be reprogrammed to acquire Th2 cytokine memory and vice versa. The capacity for reprogramming appears not to be symmetric; in some settings, Th1-to-Th2 conversion is more readily achieved than the opposite process (Löhning et al., 2002). Plasticity is lost if the cells are subjected to the same type of differentiation conditions repeatedly (Murphy et al., 1996; Sornasse et al., 1996; Assenmacher et al., 1998; Hu-Li et al., 1997; Löhning et al., 2002). The mechanisms underlying plasticity and stabilization of cytokine memory are of great interest for the understanding of decision making in the immune system and of potential practical relevance for the diagnosis and therapy of immune disorders.

In Th1 development there are master regulators that could play a similar role as GATA-3 in the Th2 pathway. The prime candidate for such a role is the T-box transcription factor T-bet that is

differentially upregulated by Th1-polarizing stimuli (Szabo et al., 2000). When expressed ectopically in cells not otherwise subjected to Th1 conditions, T-bet can induce the Th1 cytokine profile. Several studies indicate that there are cell-intrinsic interactions of the Th1 and Th2 regulators. First, GATA-3 expression is downregulated in Th1 cells below the basal level seen in naive Th cells, suggesting repression of GATA-3 expression by a Th1-specific mechanism (Zhang et al., 1997). Second, ectopic expression of GATA-3 in Th1 cells downregulates the Th1 master factor T-bet, pointing to a reciprocal inhibition of T-bet by a Th2-specific mechanism (Usui et al., 2003). In addition, the question whether T-bet also exhibits autoactivation has recently received great attention. Mullen et al. (2001) have proposed a cell-intrinsic T-bet autoactivation mechanism. However, Afkarian et al. (2002) have provided evidence that T-bet autoactivation arises from an autocrine feedback loop that operates via secretion of the cytokine IFN- $\gamma$  and not from direct intracellular feedback. As cytokine secretion is a transient phenomenon, an autocrine loop will not be sufficient to establish persistent memory expression of T-bet. This is different from GATA-3 expression, where a memory effect can arise from the direct, cell-intrinsic autoactivation (Ouyang et al., 2000; Farrar et al., 2001; Höfer et al., 2002). An autocrine positive feedback also exists in the case of GATA-3 (via secreted IL-4) but, in agreement with the results from our model, it is not required for GATA-3 memory expression (Ouyang et al., 2000).

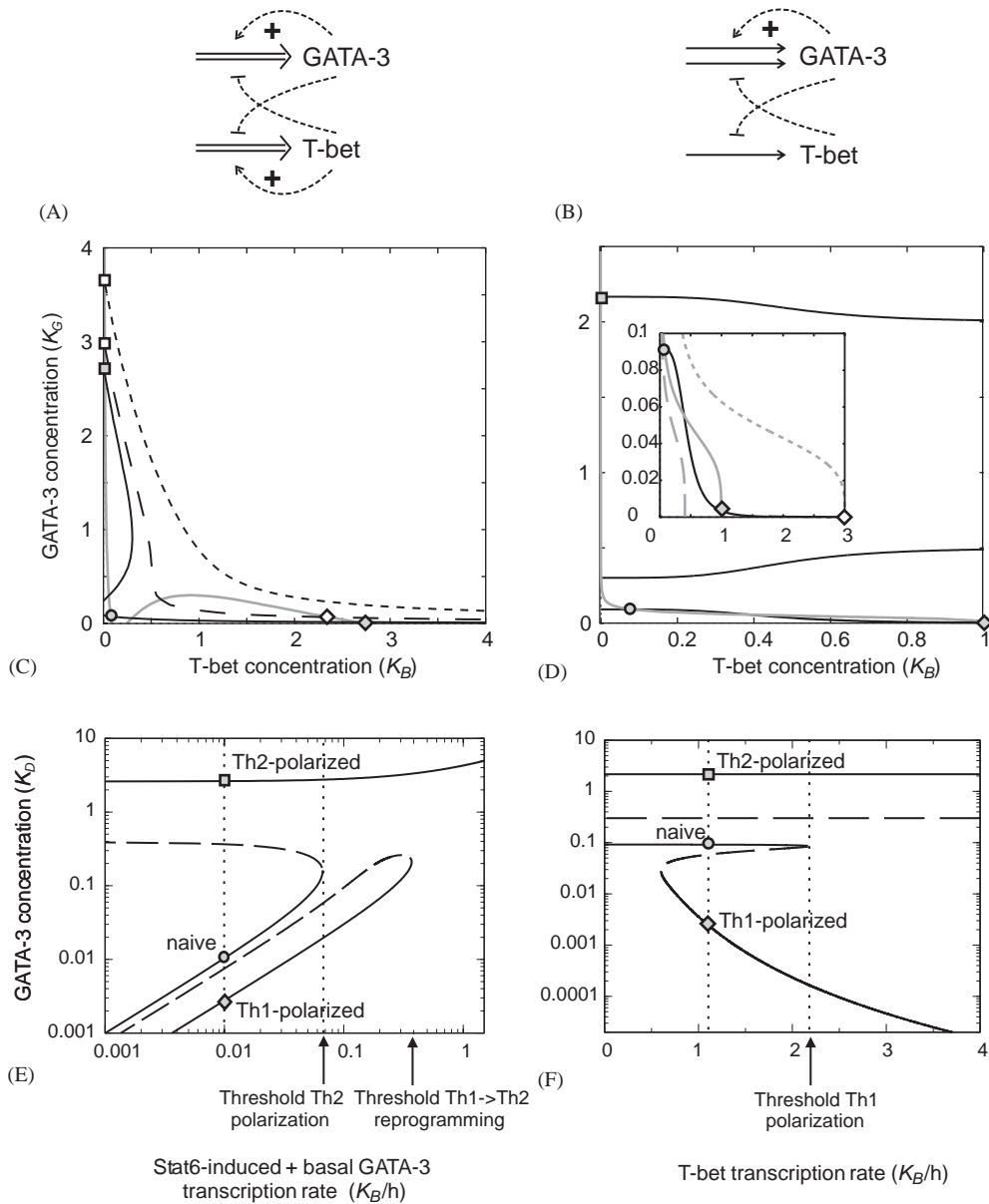
Based on our findings on repression mechanisms of GATA-3 we have developed models that include cell-intrinsic reciprocal inhibition of Th1 and Th2 pathways. As shown in the previous section, two modes of GATA-3 inhibition can account for the downregulation of basal GATA-3 expression: repression of basal GATA-3 transcription alone, and global repression of GATA-3 transcription affecting both the basal rate and autoactivation. For T-bet similar issues may arise, depending on whether it exhibits cell-intrinsic autoactivation or not. We have analyzed all the possible models, with different modes of mutual inhibition between Th1 and Th2 pathways, and with and without T-bet autoactivation. In the following we will discuss the behavior of two models that represent extreme cases. In the first—symmetric—model, we assume that both GATA-3 and T-bet are autoactivated and that each factor inhibits basal expression and autoactivation of the other, possibly through downstream mechanisms (Fig. 11A; interestingly, this regulatory scheme has also been proposed for two master regulators of muscle differentiation, myo-D and myf-5; Wolpert et al., 2002). In the second—asymmetric—model, we assume that only GATA-3 shows autoactivation, a Th1-specific mechanism represses the basal expression of GATA-3 but not autoactivation, and a Th2-specific mechanism represses T-bet expression (Fig. 11B). The mathematical formulation of the two models is given in Appendix B.

### 3.3.1. Symmetric model of master transcription factors

When T-bet exhibits autoactivation in a similar fashion as GATA-3, then it can also have two distinct expression states, with a switch from low expression to sustained high, autoactivated, expression triggered by external Th1-polarizing stimuli. Coupling both GATA-3 and T-bet reciprocally by sufficiently strong inhibition (see Eqs. (2.16) and (2.17)), the possible steady states are obtained graphically in a similar fashion as shown in Section 2.2. The dependence of GATA-3 on T-bet-mediated repression is given by Fig. 10B, which is now mirrored by a similar curve for T-bet repression mediated by GATA-3, resulting in Fig. 11C. It can be shown that this diagram, reflecting the symmetry of the model assumptions, is obtained under quite general conditions on the system parameters. Therefore, we have three stable steady states: low GATA-3 and low T-bet

concentrations (Fig. 11C, gray circle), high T-bet and low GATA-3 concentrations (Fig. 11C, gray diamond), and high GATA-3 and low T-bet concentrations (Fig. 11C, gray square). These states correlate qualitatively with the expression patterns found in naive, Th1 cells, and Th2 cells, respectively. The primary effect of the cross-inhibition is the suppression of a state in which both GATA-3 and T-bet show high expression.

In a similar fashion as done for the GATA-3 model, the effects of external stimulation with Th1-polarizing or Th2-polarizing stimuli can be evaluated. A Th2-polarizing stimulus results in a shift of the GATA-3 expression curve upwards (Fig. 11C, long-dashed line), such that the naive



state disappears and the Th2 (high GATA-3) state is approached (Fig. 11C, open square above the gray square). Thus a naïve Th cell would become Th2-polarized. However, a very strong Th2-polarizing stimulus would also abolish the Th1 state (Fig. 11C, short-dashed line), which would result in the reprogramming of a Th1-polarized cell into a Th2-polarized cell. Such reprogramming can indeed be observed experimentally (Murphy et al., 1996; Assenmacher et al., 1998; Löhning et al., 2002). The effects of a Th2-polarizing stimulus are summarized in Fig. 11E; it can be seen that there is a threshold for polarization of naïve cells and a higher threshold for the reprogramming of Th1 cells. Because of the symmetry of the model, the response-curve for a Th1-polarizing stimulus has the same form, with Th1 and Th2 branches being exchanged.

### 3.3.2. Asymmetric model of master transcription factors

In the asymmetric model, the induction of Th2 memory can again rely on GATA-3 autoactivation, whereas a transcriptional Th1 memory cannot be induced in the same manner because there is no cell-intrinsic T-bet autoactivation (Fig. 11B). Therefore the question arises whether in this model there can be alternative transcriptional mechanisms for Th1 memory. We found that this can be the case if the reciprocal repression between Th1 and Th2 pathways is already effective in naïve cells, and in this case the model yields particularly interesting results. Th1 memory can be shown to require two conditions on the parameters of repression: (i) the GATA-3-mediated repression of T-bet sets in at a lower GATA-3 concentration than GATA-3 autoactivation, and (ii) both GATA-3 and T-bet repression responses are sigmoid (compare Section 2.2, subsection *Cross-inhibition*). Then we obtain a steady-state diagram that combines

Fig. 11. Hypothetical model of the interaction of Th1 and Th2 master transcription factors. T-bet is considered as a Th1 counterpart of GATA-3 in Th2 cells. However, further factors could participate in the regulatory loops described. (A) Symmetric model: Like GATA-3, also T-bet is subject to direct autoactivation (as proposed by Mullen et al., 2001). GATA-3 and T-bet inhibit each other's transcription. (B) Alternative asymmetric model in which direct autoactivation is restricted to GATA-3, which also inhibits T-bet expression. T-bet inhibits basal GATA-3 expression but not autoactivation. This model follows from the experimental results of Afkarian et al. (2002). (C) Steady states of GATA-3 and T-bet expression in the symmetric model determined in the same manner as shown in Fig. 4C. The intersection between GATA-3 and T-bet steady-state lines (solid black and gray curves, respectively), yields three stable steady states, corresponding to naïve (gray circle), Th1-polarized (gray diamond), and Th2 polarized (gray square) states. Stat6-induced GATA-3 transcription shifts the GATA-3 steady-state line (long dashed line), such that the naïve state disappears—the system would then switch to the Th2-polarized state. A further increase in Stat6-induced GATA-3 transcription (short-dashed line) causes also the Th1 state to disappear, corresponding to a reprogramming from Th1-polarized to Th2-polarized cells. As the model is symmetric, the same effects would be observed when T-bet expression is activated by external signals. (D) The corresponding diagram for the asymmetric model shows again stable naïve (circle), Th1-polarized (diamond) and Th2-polarized (square) states; note the blow-up in the inset. An increase in Stat6-induced GATA-3 transcription has very similar effects as discussed in (C). Because of the asymmetry, however, an increase in T-bet transcription by external signals (dotted gray line in the inset) can abolish the naïve state but not the Th2-polarized state. (E) Stimulus-response diagram of GATA-3 versus a Stat6 stimulus calculated for the symmetric model. One observes the above-described three stable states and two thresholds—one for initial Th2 polarization of naïve cells and another for the Th2-reprogramming of Th1-polarized cells. (F) Stimulus-response diagram of GATA-3 versus an external T-bet-activating stimulus for the asymmetric model. Th1-polarization from the naïve state occurs beyond the bifurcation point indicated. However, in contrast to the symmetric model, the Th2-polarized state can no longer be reprogrammed to a Th1 state. Dashed lines in E and F mark unstable states. For further details see Appendix B.

bistability achieved by mutual repression between T-bet and GATA-3 pathways (see Fig. 4) and bistability achieved by GATA-3 autoactivation (Fig. 11D), yielding again three stable states: low T-bet and basal GATA-3 concentrations (naïve), high T-bet and downregulated GATA-3 concentrations (Th1-polarized), and upregulated (autoactivated) GATA-3 and low T-bet concentrations (Th2-polarized).

In this system, the basal levels of GATA-3 in a naïve Th cell are assumed to cause, in a direct manner or through a downstream mechanism, sufficient repression of T-bet (Fig. 11D, circle). Th1-polarizing signals would activate T-bet which thereby overcomes its repression and now itself inactivates GATA-3 in a Th1-polarized state (Fig. 11D, gray diamond). Conversely, Th2-polarizing signals would switch on GATA-3 autoactivation leading to stable GATA-3 upregulation, and T-bet expression would remain switched off in this Th2-polarized state (Fig. 11D, gray square).

Analysis of the responses to external signals shows that Th1- and Th2-polarizing stimuli have different effects; Th2-polarization is again possible from the naive state. Similarly, a Th1-polarizing stimulus can induce the Th1-polarized state from the naive state. Once the Th1-polarized state is reached, it can still be reprogrammed into the Th2-polarized state by strong Th2 stimulation, much in the same way as shown in Fig. 11E for the symmetric model. However, a Th2-polarized cell cannot be reprogrammed by a Th1-polarizing stimulus. This is seen in the stimulus-response diagram of Fig. 11F: the steady-state branch corresponding to Th2-polarization with high GATA-3 is not destabilized by Th1 stimuli, which contrasts with the destabilization of the Th1-polarization branch at the reprogramming threshold in Fig. 11E. Mechanistically, this is due to the assumption that basal and Stat6-induced GATA-3 transcription are subject to inhibition by the Th1 pathway, whereas GATA-3 autoactivation is not.

Thus the asymmetry of the model assumptions translates into asymmetry of the reprogramming behavior. Autoactivation of GATA-3 provides stability of Th2-polarization, whereas T-bet regulation exhibits plasticity and is susceptible to the adverse, Th2-polarizing, signals. There are indeed experimental observations that point to greater plasticity of Th1 memory compared to Th2 memory (Hu-Li et al., 1997; Afkarian et al., 2002). However, also Th1 memory can be stabilized by repetitive stimulations under Th1-inducing conditions (Murphy et al., 1996; Assenmacher et al., 1998); and Th2 memory may also exhibit some initial plasticity (Smits et al., 2001).

#### 4. Conclusions

In this paper, we have analyzed transcriptional regulatory networks of differentiation in Th lymphocytes. Our starting point were experimental observations showing that the master regulator of Th2 development, GATA-3, is an autoactivating transcription factor (Ouyang et al., 2000). Transcriptional autoactivation has been suggested as a fundamental mechanism for establishing stable cell differentiation (Wolpert et al., 2002). The wealth of data that has become available on the regulation of GATA-3 allows detailed questions to be asked on how autoactivation can cause transcriptional imprinting, and on how this mechanism can be integrated in regulatory networks that mediate differentiation responses to external stimuli (Löhning et al., 2002; Murphy and Reiner, 2002). To be able to investigate the properties of such networks quantitatively, we have developed and analysed mathematical models.

The response curve for autoactivation plays a crucial role for its regulation by external signals. If the transcription rate is a sigmoid function of the autoactivator concentration, bistability is obtained that equips the system with intrinsic thresholds for the response to signals. It is noteworthy that all the individual components of the system exhibit smooth response kinetics; the sharp thresholds arise from their interaction. To uncover such properties, mathematical analysis of the system behavior is necessary. Specifically, the coexistence of stable low-expression and high-expression states in the dynamical system implies that no inhibitory mechanism is needed to contain spontaneous autoactivation. When the system is in the low-expression state, the autoactivation loop can be switched on only by further external stimulation of autoactivator expression. In this way transient differentiation signals will be memorized.

Inhibitors extend the regulatory potential of the system. We have shown how different molecular mechanisms of inhibition may attenuate the system's response to external signals or extinguish an established autoactivation loop. However, the signature of the intrinsic bistability is also present in the responses to inhibitors, such that the theoretically obtained titration curves of inhibitors exhibit sharp thresholds. Because of this property, the effect of an inhibitor is expected to strongly depend on its expression level. The theoretical predictions made in this study are relevant for elucidating the mechanisms of factors that have recently been implicated in inhibition of GATA-3, including FOG-1, ROG, Runx-1, and Bcl6 (Zhou et al., 2001; Kurata et al., 2002; Komine et al., 2003; Kusam et al., 2003).

Reciprocal inhibitory interactions have been suggested to occur between the major alternative differentiation pathways of Th cells, Th1 and Th2, and several experimental observations support this notion. However, very little is currently known on the molecular mechanisms that could form such a regulatory network. We have extended our model of GATA-3 regulation to include a Th1 master factor, likely to be T-bet, and analyzed hypothetical interaction networks which share the common feature of cross-inhibition between Th1 and Th2 master factors and GATA-3 autoactivation. When autoactivation of T-bet is assumed (Mullen et al., 2001), a network with symmetric regulation of Th1 and Th2 differentiation by Th1-polarizing and Th2-polarizing stimuli can result. In contrast, when cell-intrinsic T-bet autoactivation is absent, as has been implicated by recent experimental results (Afkarian et al., 2002), Th2 differentiation is found to be more stable than Th1 differentiation. It is important to note that these results do not depend on whether the hypothesized reciprocal inhibition of GATA-3 and T-bet is direct or occurs through intermediate factors.

A model without cell-intrinsic T-bet autoactivation raises the question of how a Th1 cell fate is imprinted on a molecular level. In the asymmetric model we presented, it has been shown that stable transcriptional imprinting can also be based on reciprocal inhibitory interactions with Th2 regulators, such that sustained high levels of T-bet (or, possibly, of another Th1 master regulator) would result from the release of inhibition. A prediction of this model is that GATA-3 is already present in naive Th cells, and decreases in Th1 cells, which is in agreement with the available data. Inhibition of T-bet has recently been demonstrated by retroviral GATA-3 transduction, but molecular mechanisms have not been fully elucidated (Usui et al., 2003).

An alternative hypothesis would be that Th1 differentiation is not mediated by stable transcriptional imprinting. Instead, the transient, stimulation-dependent elevation of Th1 factors such as T-bet, or the inhibition of GATA-3, or both, may directly be translated into rather stable epigenetic modifications of cytokine genes and of the genes encoding the regulators of cytokine

expression. The reciprocal epigenetic regulation of cytokine loci, with opening of the Th2 and closing of the Th1 cytokine genes in Th2 cells, and vice versa in Th1 cells, is a well-documented and currently intensely studied process (Löhning et al., 2002; Murphy and Reiner, 2002; Ansell et al., 2003). The coordination of the molecular mechanisms involved, such as changes in DNA methylation and histone acetylation, by signaling networks presents a fundamental open question. The observation that changes in the master transcription factors GATA-3, T-bet, and others precede detectable chromatin modifications along the differentiation pathways of Th cells, would be suggestive of a hierarchical regulation. Indeed, GATA-3 has been shown experimentally to mediate chromatin remodeling at the IL-4 locus (Ouyang et al., 2000). To elucidate the relationship between transcriptional and epigenetic imprinting will require knowledge on the mechanisms and, importantly, the temporal and spatial dynamics of chromatin modifications.

### Acknowledgements

Stimulating discussions with Ken Murphy and the members of the Radbruch group, and financial support from DFG (through SFB618, to T. H. and A. R.) and Ernst Schering Research Foundation (to M. L.) are gratefully acknowledged.

### Appendix A. GATA-3 repression models

To obtain a reasonably accurate description for the slow temporal dynamics observed for GATA-3, we used the version of the GATA-3 expression model given in Höfer et al. (2002), where three mRNA species (nascent transcript, processed transcript, mRNA associated with ribosomes) and three protein species (inactive cytoplasmic GATA-3, active cytoplasmic GATA-3, and active nuclear GATA-3) were assumed. The steady states of this model are identical to the simplified model given in Section 3.1.

The sponge repressor ( $R_1$ ) was taken to act on the nuclear protein concentration,  $G_n$ , by adding the term

$$f(I, G_n) = -k_{\text{on}}(I_{\text{tot}} - I)G_n + k_{\text{off}}I$$

to the kinetic equation for  $G_n$  (see Höfer et al., 2002) and writing the kinetic equation for the concentration of the inactive repressor–GATA-3 complex

$$\frac{dI}{dt} = -f(I, G_n).$$

$I_{\text{tot}}$ ,  $k_{\text{on}}$ , and  $k_{\text{off}}$  denote the total repressor concentration, and its on and off rate constants for GATA-3 binding. Assuming the repressor to act in the cytoplasmic compartment gave very similar results. We assumed a dissociation constant  $k_{\text{off}}/k_{\text{on}} = 0.1$ . in units of GATA-3 concentration and reasonably fast binding and dissociation compared to the GATA-3 kinetics ( $k_{\text{off}} = 10/h$ ). In Fig. 9, we give the dimensionless ratio of the total repressor concentration to the dissociation constant  $I_{\text{tot}}/(k_{\text{off}}/k_{\text{on}})$ .

To account for the repressors of basal transcription and GATA-3 autoactivation ( $R_2$  and  $R_3$  in Fig. 8), we modified the GATA-3 transcription term to read

$$g(I)v_{\text{ext}} + v_{\text{max},G} \left( \frac{G}{K_G + G} \right)^2 \quad \text{and} \quad v_{\text{ext}} + g(I)v_{\text{max},G} \left( \frac{G}{K_G + G} \right)^2,$$

respectively, where

$$g(I) = \frac{1}{1 + I/K_I}$$

with the repressor concentration  $I$  and dissociation (inhibitor) constant  $K_I$ .

## Appendix B. Equations for the GATA-3 T-bet cross-regulation models

Following the assumptions discussed in Section 3.3, the symmetric cross-regulation model (Fig. 11A) was described by

$$\begin{aligned} \frac{dR_G}{dt} &= \frac{v_{\text{ext},G} + v_{\text{max},G} \left( \frac{G}{K_G + G} \right)^2}{1 + B/L_B} - k_R R_G, & \frac{dG}{dt} &= k_t R_G - k_p G, \\ \frac{dR_B}{dt} &= \frac{v_{\text{ext},B} + v_{\text{max},B} \left( \frac{B}{K_B + B} \right)^2}{1 + G/L_G} - k'_R R_B, & \frac{dB}{dt} &= k'_t R_B - k'_p B, \end{aligned}$$

where  $R_G$  and  $R_B$  denote the concentrations of GATA-3 and T-bet mRNA, respectively, while  $G$  and  $B$  stand for the respective protein concentrations.  $L_B$  and  $L_G$  are the inhibition constants for T-bet on GATA-3 transcription and GATA-3 on T-bet transcription, respectively. The system was non-dimensionalized and analyzed for varying parameter values. It was assumed that the effective concentrations of GATA-3 and T-bet for autoactivation and mutual inhibition were in the same range. Then the behavior depicted in Figs. 11C and E is characteristic for a wide range of parameter values. For simplicity, we took  $K_G = K_B = L_G = L_B = 1$ ,  $v_{\text{max},G} = 5/h$ ,  $v_{\text{max},B} = 5/h$ ,  $k_R = k'_R = k_t = k'_t = k_p = k'_p = 1/h$ , and varied only the external-stimulus-induced transcription rates  $v_{\text{ext},G}$  and  $v_{\text{ext},B}$ .

The asymmetric cross-regulation model (Fig. 11B) reads

$$\begin{aligned} \frac{dR_G}{dt} &= \frac{v_{\text{ext},G}}{1 + (B/L_B)^4} + v_{\text{max},G} \left( \frac{G}{K_G + G} \right)^2 - k_R R_G, & \frac{dG}{dt} &= k_t R_G - k_p G, \\ \frac{dR_B}{dt} &= \frac{v_{\text{ext},B}}{1 + (G/L_G)^4} - k'_R R_B, & \frac{dB}{dt} &= k'_t R_B - k'_p B. \end{aligned}$$

In contrast to the symmetric model, T-bet is no longer taken to be subject to direct autoactivation and is assumed to inhibit only basal and Stat6-induced GATA-3 transcription. Under the assumptions of (i) steep inhibition responses (Hill coefficients of four) and (ii) of GATA-3-mediated T-bet repression operating at lower GATA-3 concentrations than GATA-3

autoactivation ( $L_G < K_G$ ), the three stable steady states as shown in Figs 11D and F were obtained. For Fig. 11D, we took  $L_G = 0.05$ ,  $L_B = 0.5$ ,  $v_{\text{ext},G} = 0.06/h$ ,  $v_{\text{ext},B} = 1/h$ ,  $v_{\text{max},G} = 4.5/h$  and all other parameters as in the symmetric model. To study the response to external stimuli,  $v_{\text{ext},G}$  and  $v_{\text{ext},B}$  were varied systematically.

## References

- Abbas, A.K., Murphy, K.M., Sher, A., 1996. Functional diversity of helper T lymphocytes. *Nature* 383, 787–793.
- Ackers, G.K., Johnson, A.D., Shea, M.A., 1982. Quantitative model for gene regulation by  $\lambda$  phage repressor. *Proc. Natl. Acad. Sci. USA* 79, 1129–1133.
- Afkarian, M., Sedy, J.R., Yang, J., Jacobson, N.G., Cereb, N., Yang, S.Y., Murphy, T.L., Murphy, K.M., 2002. T-bet is a STAT1-induced regulator of IL-12R expression in naive CD4(+) T cells. *Nat. Immunol.* 3, 549–557.
- Ansel, K.M., Lee, D.U., Rao, A., 2003. An epigenetic view of helper T cell differentiation. *Nat. Immunol.* 4, 616–623.
- Arnold, H.H., Winter, B., 1998. Muscle differentiation: more complexity to the network of myogenic regulators. *Curr. Opin. Genet. Dev.* 8, 539–544.
- Asnagli, H., Afkarian, M., Murphy, K.M., 2002. Cutting edge: identification of an alternative GATA-3 promoter directing tissue-specific gene expression in mouse and human. *J. Immunol.* 168, 4268–4271.
- Assenmacher, M., Löhning, M., Scheffold, A., Richter, A., Miltenyi, S., Schmitz, J., Radbruch, A., 1998. Commitment of individual Th1-like lymphocytes to expression of IFN-gamma versus IL-4 and IL-10: selective induction of IL-10 by sequential stimulation of naive Th cells with IL-12 and IL-14. *J. Immunol.* 161, 2825–2832.
- Bar-Or, R.L., Maya, R., Segel, L.A., Alon, U., Levine, A.J., Oren, M., 2000. Generation of oscillations by the p53-Mdm2 feedback loop: a theoretical and experimental study. *Proc. Natl. Acad. Sci. USA* 97, 11250–11255.
- Chen, C.H., Zhang, D.H., LaPorte, J.M., Ray, A., 2000. Cyclic AMP activates p38 mitogen-activated protein kinase in Th2 cells: phosphorylation of GATA-3 and stimulation of Th2 cytokine gene expression. *J. Immunol.* 165, 5597–5605.
- Cosma, M.P., 2002. Ordered recruitment: gene-specific mechanism of transcription activation. *Mol. Cell* 10, 227–236.
- Das, J., Chen, C.H., Yang, L.Y., Cohn, L., Ray, P., Ray, A., 2001. A critical role for NF-kappa B in Gata3 expression and T(H)2 differentiation in allergic airway inflammation. *Nat. Immunol.* 2, 45–50.
- Dundr, M., Hoffmann-Rohrer, U., Hu, Q., Grummt, I., Rothblum, L.I., Phair, R.D., Mistelli, T., 2002. A kinetic framework for mammalian RNA polymerase in vivo. *Science* 298, 1623–1626.
- Farrar, J.D., Ouyang, W., Löhning, M., Assenmacher, M., Radbruch, A., Kanagawa, O., Murphy, K.M., 2001. An instructive component in T helper cell type 2 (Th2) development mediated by GATA-3. *J. Exp. Med.* 193, 643–649.
- George, K.M., Leonard, M.W., Roth, M.E., Lieu, K.H., Kioussis, D., Grosveld, F., Engel, J.D., 1994. Embryonic expression and cloning of the murine GATA-3 gene. *Development* 120, 2673–2686.
- Gregoire, J.M., Romeo, P.H., 1999. T-cell expression of the human GATA-3 gene is regulated by a non-lineage-specific silencer. *J. Biol. Chem.* 274, 6567–6578.
- Goldbeter, A., 1996. *Biochemical Oscillations and Cellular Rhythms*. Cambridge University Press, Cambridge.
- Goodwin, B.C., 1963. *Temporal organisation in cells: a dynamic theory of cellular control processes*. Academic Press, New York.
- Hasty, J., McMillen, D., Isaacs, F., Collins, J.J., 2001. Computational studies of gene regulatory networks: in numero molecular biology. *Nat. Rev. Genet.* 2, 268–279.
- Heinrich, R., Schuster, S., 1996. *The Regulation of Cellular Systems*. Chapman & Hall, New York.
- Heinrich, R., Rapoport, S.M., Rapoport, T.A., 1977. Metabolic regulation and mathematical models. *Prog. Biophys. Mol. Biol.* 32, 1–82.
- Hirate, H., Yoshiura, S., Ohtsuka, T., Bessho, Y., Harada, T., Yoshikawa, K., Kageyama, R., 2002. Oscillatory expression of the bHLH factor Hes1 regulated by a negative feedback loop. *Science* 298, 840–843.
- Höfer, T., Nathansen, H., Löhning, M., Radbruch, A., Heinrich, R., 2002. GATA-3 transcriptional imprinting in Th2 lymphocytes: a mathematical model. *Proc. Natl. Acad. Sci. USA* 99, 9364–9368.

- Hoffmann, A., Levchenko, A., Scott, M.L., Baltimore, D., 2002. The I $\kappa$ B-NF- $\kappa$ B signaling module: temporal control and selective gene activation. *Science* 298, 1241–1245.
- Hu-Li, J., Huang, H., Ryan, J., Paul, W.E., 1997. In differentiated CD(+) T cells, interleukin 4 production is cytokine-autonomous, whereas interferon gamma production is cytokine-dependent. *Proc. Natl. Acad. Sci. USA* 94, 3189–3194.
- Hu-Li, J., Pannetier, C., Guo, L.Y., Löhning, M., Gu, H., Watson, C., Assenmacher, M., Radbruch, A., Paul, W.E., 2001. Regulation of expression of IL-4 alleles: analysis using a chimeric GFP/IL-4 gene. *Immunity* 14, 1–11.
- Hunding, A., 1974. Limit cycles in enzyme systems with non-linear negative feedback. *Biophys. Struct. Mechan.* 1, 47–54.
- de Jong, H., 2002. Modeling and simulation of genetic regulatory systems: a literature review. *J. Comput. Biol.* 9, 67–103.
- Kimura, H., Sugaya, K., Cook, P.R., 2002. The transcription cycle of RNA polymerase II in living cells. *J. Cell Biol.* 159, 777–782.
- Komine, O., Hayashi, K., Natsume, W., Watanabe, T., Seki, Y., Seki, N., Yagi, R., Sukzuki, W., Tamauchi, H., Hozumi, K., Habu, S., Kubo, M., Satake, M., 2003. The Runx1 transcription factor inhibits the differentiation of naive CD4+ T cells into the Th2 lineage by repressing GATA3 expression. *J. Exp. Med.* 198, 51–61.
- Kurata, H., Lee, H.J., O'Garra, A., Arai, N., 1999. Ectopic expression of activated Stat6 induces the expression of Th2-specific cytokines and transcription factors in developing Th1 cells. *Immunity* 11, 677–688.
- Kurata, H., Lee, H.J., McClanahan, T., Coffman, R.L., O'Garra, A., Arai, N., 2002. Friend of GATA is expressed in naive Th cells and functions as a repressor of GATA3-mediated Th2 cell development. *J. Immunol.* 168, 4538–4545.
- Kusam, S., Toney, L.M., Sato, H., Dent, A.L., 2003. Inhibition of Th2 differentiation and GATA-3 expression by BCL-6. *J. Immunol.* 170, 2435–2441.
- Lavenu-Bombled, C., Trainor, C.D., Makeh, I., Romeo, P.H., Max-Audit, I., 2002. Interleukin-13 gene expression is regulated by GATA-3 in T cells—role of a critical association of a GATA and two GATG motifs. *J. Biol. Chem.* 277, 18313–18321.
- Lewis, J., 2003. Autoinhibition with transcriptional delay: a simple mechanism for the zebrafish somitogenesis oscillator. *Curr. Biol.* 13, 1398–1408.
- Löhning, M., Richter, A., Radbruch, A., 2002. Cytokine memory of T helper lymphocytes. *Adv. Immunol.* 80, 115–181.
- Lun, Y., Sawadogo, M., Perry, M., 1997. Autoactivation of *Xenopus* MyoD transcription and its inhibition by USF. *Cell. Growth Differ.* 8, 275–282.
- Markevich, N.I., Hoek, J.B., Kholodenko, B.N., 2004. Signaling switches and bistability arising from multisite phosphorylation in protein kinase cascades. *J. Cell Biol.* 164, 353–359.
- Miaw, S.C., Choi, A., Yu, E., Kishikawa, H., Ho, I.C., 2000. ROG, repressor of GATA, regulates the expression of cytokine genes. *Immunity* 12, 323–333.
- Monk, N.A.M., 2003. Oscillatory expression of Hes1, p53, and NF-kappa B driven by transcriptional time delays. *Curr. Biol.* 13, 1409–1413.
- Mullen, A.C., High, F.A., Hutchins, A.S., Lee, H.W., Villarino, A.V., Livingston, D.M., Kung, A.L., Cereb, N., Yao, T.P., Yang, S.Y., Reiner, S.L., 2001. Role of T-bet in commitment of T(H)1 cells before IL-12-dependent selection. *Science* 292, 1907–1910.
- Murphy, E., Shibuya, K., Hosken, N., Openshaw, P., Maino, V., Davis, K., Murphy, K., O'Garra, A., 1996. Reversibility of T helper 1 and 2 populations is lost after long-term stimulation. *J. Exp. Med.* 183, 901–913.
- Murphy, K.M., Reiner, S.L., 2002. The lineage decisions of helper T cells. *Nat. Rev. Immunol.* 2, 933–944.
- Ouyang, W., Ranganath, S.H., Weindel, K., Bhattacharya, D., Murphy, T.L., Sha, W.C., Murphy, K.M., 1998. Inhibition of Th1 development mediated by GATA-3 through an IL-4-independent mechanism. *Immunity* 9, 745–755.
- Ouyang, W., Löhning, M., Gao, Z., Assenmacher, M., Ranganath, S., Radbruch, A., Murphy, K.M., 2000. Stat6-independent GATA-3 autoactivation directs IL-4-independent Th2 development and commitment. *Immunity* 12, 27–37.
- Radbruch, A., Tykocinski, L., Hajkova, P., Stamm, T., Soezeri, O., Löhning, M., Friedrich, B., Hu-Li, J., Pannetier, C., Paul, W.E., Gruetz, G., Walter, J., 2002. A GATA-3 binding site in the first intron of the interleukin-4 gene defines a critical element for the memory expression of interleukin-4 in Th lymphocytes. *Arthritis Rheum.* 46, S399.

- Rhodes, S.J., Chen, R., DiMattia, G.E., Scully, K.M., Kalla, K.A., Lin, S.C., Yu, V.C., Rosenfeld, M.G., 1993. A tissue-specific enhancer confers Pit-1-dependent morphogen inducibility and autoregulation on the pit-1 gene. *Genes Dev.* 7, 913–932.
- Salazar, C., Höfer, T., 2003. Allosteric regulation of the transcription factor NFAT1 by multiple phosphorylation sites: a mathematical analysis. *J. Mol. Biol.* 327, 31–45.
- Schellenberger, W., Hervagault, J.F., 1991. Irreversible transitions in the 6-phosphofructokinase/fructose 1,6-bisphosphatase cycle. *Eur. J. Biochem.* 195, 109–113.
- Setty, Y., Mayo, A.E., Surette, M.G., Alon, U., 2003. Detailed map of a cisregulatory input function. *Proc. Natl. Acad. Sci. USA* 100, 7702–7707.
- Siegel, M.D., Zhang, D.H., Ray, A., 1995. Activation of the interleukin-4 promoter by cAMP in murine EL-4 cells requires the GATA-3 and Cleo elements. *J. Biol. Chem.* 270, 24548–24555.
- Smits, H.H., van Rietschoten, J.G.I., Hilkens, C.M.U., Sayilir, R., Stiekema, F., Kapsenberg, M.L., Wierenga, E.A., 2001. IL-12-induced reversal of human Th2 cells is accompanied by full restoration of IL-12 responsiveness and loss of GATA-3 expression. *Eur. J. Immunol.* 31, 1055–1065.
- Sornasse, T., Larenas, P.V., Davis, K.A., de Vries, J.E., Yssel, H., 1996. Differentiation and stability of T helper 1 and 2 cells derived from naive human neonatal CD4+ T cells, analyzed at the single-cell level. *J. Exp. Med.* 184, 473–483.
- Strogatz, S., 1994. *Nonlinear Dynamics and Chaos*. Addison-Wesley, Reading, MA.
- Szabo, S.J., Kim, S.T., Costa, G.L., Zhang, X.K., Fathman, C.G., Glimcher, L.H., 2000. A novel transcription factor, T-bet, directs Th1 lineage commitment. *Cell* 100, 655–669.
- Thomas, R., Thieffry, D., Kaufman, M., 1995. Dynamical behaviour of biological regulatory networks—I. Biological role of feedback loops and practical use of the concept of the loop-characteristic state. *Bull. Math. Biol.* 57, 247–276.
- Tsai, S.F., Strauss, E., Orkin, S.H., 1991. Functional analysis and in vivo footprinting implicate the erythroid transcription factor GATA-1 as a positive regulator of its own promoter. *Genes Dev.* 5, 919–931.
- Tsang, A.P., Visvader, J.E., Turner, C.A., Fujiwara, Y., Yu, C., Weiss, M.J., Crossley, M., Orkin, S.H., 1997. FOG, a multitype zinc finger protein, acts as a cofactor for transcription factor GATA-1 in erythroid and megakaryocytic differentiation. *Cell* 90, 109–119.
- Tyson, J.J., Othmer, H.G., 1978. The dynamics of feedback control circuits in biochemical pathways. *Prog. Theor. Biol.* 5, 1–62.
- Usui, T., Nishikomori, R., Kitani, A., Strober, W., 2003. GATA-3 suppresses Th1 development by downregulation of Stat4 and not through effects on IL-12R beta 2 chain or T-bet. *Immunity* 18, 415–428.
- Wolpert, L., Beddington, R., Jesell, T., Lawrence, P., Meyerowitz, E., Smith, J., 2002. *Principles of Development*, 2nd Edition. Oxford University Press, Oxford.
- Xiong, W., Ferrell Jr., J.E., 2004. A positive-feedback-based bistable ‘memory module’ that governs a cell fate decision. *Nature* 426, 460–465.
- Yamagata, T., Mitani, K., Oda, H., Suzuki, T., Honda, H., Asai, T., Maki, K., Nakamoto, T., Hirai, H., 2000. Acetylation of GATA-3 affects T-cell survival and homing to secondary lymphoid organs. *EMBO J.* 19, 4676–4687.
- Zhang, D.H., Cohn, L., Ray, P., Bottomly, K., Ray, A., 1997. Transcription factor GATA-3 is differentially expressed murine Th1 and Th2 cells and controls Th2-specific expression of the interleukin-5 gene. *J. Biol. Chem.* 272, 21597–21603.
- Zheng, W.P., Flavell, R.A., 1997. The transcription factor GATA-3 is necessary and sufficient for Th2 cytokine gene expression in CD4 T cells. *Cell* 89, 587–596.
- Zhou, M.X., Ouyang, W., Gong, Q., Katz, S.G., White, J.M., Orkin, S.H., Murphy, K.M., 2001. Friend of GATA-1 represses GATA-3-dependent activity in CD4(+) T cells. *J. Exp. Med.* 194, 1461–1471.